Journal of Power Sources 436 (2019) 226879

Contents lists available at ScienceDirect

Journal of Power Sources

journal homepage: www.elsevier.com/locate/jpowsour

Review article

A survey of methods for monitoring and detecting thermal runaway of lithium-ion batteries

Zhenghai Liao [a,b], Shen Zhang [c], Kang Li [b], Guoqiang Zhang [a,b,*], Thomas G. Habetler [c]

[a] Institute of Electrical Engineering, Chinese Academy of Sciences, Beijing, 100190, China
[b] University of Chinese Academy of Sciences, Beijing, 100039, China
[c] School of Electrical and Computer Engineering, Georgia Institute of Technology, Atlanta, GA 30332, USA

HIGHLIGHTS

- Summarized methods monitoring and detecting thermal runaway of lithium-ion batteries.
- Elaborated the electrochemical impedance spectroscopy analysis method in detail.
- Reviewed methods of thermal runaway monitoring based on gas detection.
- Summarized methods mitigating thermal runaway at the cell level.
- Discussed the heat dissipation technology and heat isolation technology.

ARTICLE INFO

Keywords:
Lithium-ion batteries
Thermal runaway
Monitoring and detection
Sensor measurement
Protection
Application safety

ABSTRACT

Lithium-ion batteries have many advantages such as the high specific energy, the high specific power, the long calendar life, being environmentally friendly, and can be used without the memory effect. Thus this type of battery is widely used as the core component in many applications such as electric vehicles, portable electronic devices, and distributed energy storage systems. However, lithium-ion batteries can easily develop into thermal runaways due to the stress and abuse from mechanical, electrical, and thermal perspectives, posing a major threat to the overall safety of many battery systems. On the premise of passing the manufacturer's safety inspections, a variety of methods for monitoring and detecting thermal runaway events are developed to enhance the safety and robustness of lithium-ion batteries in different application scenarios. This paper thus summarizes the existing literature on this topic and presents a comparative study on the sensitivity of various monitoring and detection methods. Potential future research directions are also discussed in detail to further enhance the safety and robustness of lithium-ion battery systems.

1. Introduction

Compared to a traditional aqueous electrolyte secondary battery, a lithium-ion battery has many advantages including a higher specific energy, a higher specific power, a longer calendar life, a lower self-discharge rate, being more environmentally friendly, and can be used without the memory effect, etc [1,2]. In the 1980s, J. B. Goodenough first identified and developed Li_xCoO_2 as the cathode material and enabled the development of lithium-ion batteries, and this breakthrough ushered in the age of portable electronic devices. Since Sony corporation first launched the commercial cobaltate cathode lithium-ion battery to the market in 1991, the production process of lithium-ion batteries gradually matured and was adopted by many applications using secondary batteries [3–5]. Later, with the development and promotion of clean, renewable, and distributed energy technologies worldwide, lithium-ion batteries are being widely used as the energy storage and power supply units for essential equipments and systems such as electric vehicles, portable electronic devices, distributed chemical energy storage systems, and aerospace power systems, etc. The worldwide market value of the lithium-ion battery is growing rapidly every year, with statistics from 1992 to 2020 demonstrated in Fig. 1 [6]. However, due to the nature of many safety-critical applications, developing methodologies for monitoring and assessing the safety of lithium-ion batteries has become a major challenge for both industry and academia in recent

* Corresponding author. Institute of Electrical Engineering, Chinese Academy of Sciences, Beijing, 100190, China.
E-mail address: zhanggqi@mail.iee.ac.cn (G. Zhang).

https://doi.org/10.1016/j.jpowsour.2019.226879
Received 4 May 2019; Received in revised form 19 June 2019; Accepted 10 July 2019
Available online 20 July 2019

years.

Investigating methods to suppress the thermal runaway event is a major subject for improving the safety of lithium-ion batteries [9,10]. When a lithium-ion battery is subjected to external stress, the battery case can be either deformed or penetrated by some sharp objects, e.g., nails, causing a mechanical abuse to the lithium-ion battery. In addition, a lithium-ion battery may fail to follow its inherent electrical characteristics due to overcharging, overdischarging, and external short-circuiting, leading to an electrical abuse of the lithium-ion battery. Moreover, a lithium-ion battery can become overheated due to heat generated by an external heat source or internal electrochemical side reactions, etc., triggering a thermal abuse of the lithium-ion battery. All of these factors may cause lithium-ion batteries to undergo a series of exothermic reactions in a few minutes, leading to a drastic increase of temperature inside the battery, which may further develop into a thermal runaway event that typically leads to smoke, fire, or even explosion [11–13].

The smoke, fire, and explosion caused by a thermal runaway event are posing major threats to the lives and properties of human beings [14,15]. Nevertheless, achieving a good level of safety and reliability is now a goal for global large-scale distributed energy management systems. Therefore, to improve the safety and performance of lithium-ion batteries and mitigate concerns regarding to thermal runaway, many international organizations and commissions, i.e., the International Organization for Standardization (ISO) and the International Electrotechnical Commission (IEC), have formulated and promulgated certain authoritative test specifications to evaluate the safety of a lithium-ion battery [16,17]. These specifications require lithium-ion batteries to pass certain safety verification tests, including the overcharging test, the overdischarging test, the overheating test, and the mechanical impact test, etc., and thees regulations further require the test to not introduce any secondary hazards (leakage, fire and explosion) to the battery, thereby ensuring the quality and safety adopting lithium-ion batteries.

However, even if lithium-ion batteries could meet all of the specifications and test requirements, it's still not practical to completely eliminate the possibility of running into a thermal runaway problem, since the operating condition and the environment can be more complicated and severe when compared to many test conditions [18]. Therefore, an abuse from various sources is often inevitable. For example, in 2016, the Samsung Galaxy Note 7 caused a series of explosions all over the world due to a high probability of running into a short-circuit fault in its lithium-ion battery. Specifically, this short circuit can be introduced when there is a damage to the separator that allows the positive and negative electrodes to meet within the jellyroll, causing a substantial overheating even during normal use. In 2017, a Jiema electric bicycle caught fire and exploded due to overcharging its lithium-ion batteries. Moreover, a Tesla Model X slammed into the US 101 highway concrete divider in the San Francisco Bay Area in early 2018, causing its lithium-ion battery pack to deform and crack, which ultimately ignited the entire vehicle [9,19].

During a thermal runaway process, lithium-ion batteries may experience a voltage and current anomaly, a temperature rise, or a gas venting phenomena [20–22]. Therefore, monitoring and detecting the incipient-stage thermal runaway by measuring or estimating these characteristic signals, such as the voltage, the temperature, and the gas component, is one of the most effective methods to promote the safety of lithium-ion batteries in different application scenarios. The monitoring and detecting methods can be essentially divided into the following categories:

1) Terminal voltage detection using the battery management system (BMS);
2) Battery mechanical deformation detection using creep distance sensors;
3) Internal temperature estimation by embedding optic fiber sensors in lithium-ion batteries or monitoring the internal battery impedance change;
4) Characteristic gas component identification during the thermal runaway process.

At present, various safety issues of lithium-ion batteries in different application have been evaluated in many literature review papers, including their failure modes and mechanisms [6], their thermal safety issues [23–25], and the safety-focused modeling of the battery itself [26]. However, considering the significance and benefit of boosting the safety and robustness of lithium-ion batteries with early-warning mechanisms, there is also a strong demand to systematically review all of the papers relevant to the systems and methods for monitoring and detecting thermal runaway problems. In light of this consideration, this paper will conduct a detailed literature survey on existing methodologies monitoring and detecting a thermal runaway event, such as the terminal voltage detection method, the battery internal state monitoring

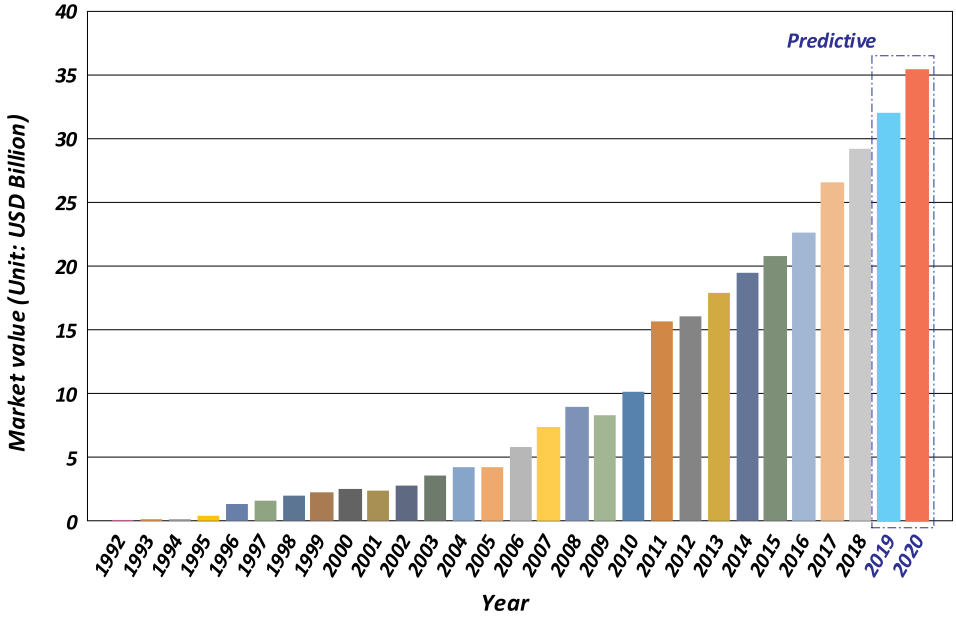

Fig. 1. Lithium-ion batteries' world market value from 1992 to 2020, with historical data from [7] and projected data from [8].

method, and the gas emission monitoring method.

The rest of this review paper is organized as follows. Sections 2 and 3 introduce the basic working principle and the thermal runaway mechanism of lithium-ion batteries. In Section 4, a detailed literature survey and discussion on thermal runaway monitoring and detecting methods is presented in detail. Subsequently, in Section 5 summarizes the protection methods against thermal runaway for lithium-ion batteries from cell-level and system-level. Section 6 concludes the paper by providing outlooks with comments and suggestion on potential research directions to further enhance the safety and robustness of lithium-ion battery systems.

2. Basic structure and working principles of lithium-ion batteries

The lithium-ion battery is a rechargeable secondary power source. Different from other secondary batteries such as the lead-acid battery or the nickel-cadmium battery, lithium-ion batteries mainly rely on the electrochemical reaction of lithium ions that migrate between the cathode and anode to charge a battery or discharge it to power an external load. A Lithium-ion battery is mainly composed of the cathode, the anode, the separator, the electrolyte, and the current collector. Various configurations also exist, such as the cylindrical battery, the prismatic battery, the coin battery, and the pouch battery, etc. [4]. This section is arranged to introduce the basic structure and working principles of lithium-ion batteries.

2.1. Cathode

The active substance of the cathode is mainly composed of lithium compounds and is required to possess a high oxidation-reduction potential, which is advantageous for increasing the battery's capacity and achieving a higher output voltage. Lithium compound materials used for the cathode mainly include the lithium iron phosphate ($LiFePO_4$) [27], the lithium nickelate ($LiNiO_2$) [28], the lithium manganate ($LiMn_2O_4$) [29], the lithium cobaltate ($LiCoO_2$) [30], the lithium nickel manganese oxide ($LiNi_{0.5}Mn_{1.5}O_2$) [31], the lithium nickel molybdenum manganese oxide ($LiNi_xMo_yMn_{1-x-y}O_2$) [32], and the lithium nickel cobalt manganese oxide ($LiNi_xCo_yMn_{1-x-y}O_2$) [33], etc. Among nickel, cobalt and manganese, nickel has the highest concentration of active substance, and the specific capacity of a lithium-ion battery increases as the density of nickel increases. The lithium-ion battery with a $LiNi_xCo_yMn_{1-x-y}O_2$ cathode has a specific capacity of 180 mAh/g when the concentration of nickel is greater than 0.5, but the excessive nickel will cause the battery capacity to decrease and the thermal stability to suffer. Fortunately, the presence of cobalt can prevent the capacity from decreasing, and the presence of manganese can improve the stability and safety of lithium-ion batteries [34–36]. It can be seen from Fig. 2 that as the concentration of nickel in the ternary material increases from 1/3 to 0.85, the specific discharge capacity would increase from 160 mAh/g to over 200 mAh/g, but its thermal stability and capacity retention rate are lowered [37]. Therefore, the study of $LiNi_xCo_yMn_{1-x-y}O_2$ has turned into a research frontier as the cathode electrode material, which aims at investigating recipes for optimizing trade-offs between the high specific energy and the insufficient thermal stability [38–42].

2.2. Anode

The active substance of the anode is required to possess a low oxidation-reduction potential, and is not subject to change with respect to the concentration of lithium intercalation. In addition, the electrochemical property of an anode's active substance must have a superior electrochemical stability and exert no impacts on the formation of the solid electrolyte interface (SEI). Since the anode of a lithium-ion battery has a low oxidation-reduction potential and relatively stable electrochemical properties, a lithium-ion battery can maintain a smooth and rapid charging and discharging capability, as well as a low self-discharge rate. The current research on the anode substance material of lithium-ion batteries are mainly focused on the lithium titanate anode ($Li_4Ti_5O_{12}$, $Ti_2Nb_{10}O_{29}$ etc.) [43–48], the carbon-based anode (graphitized carbon, amorphous carbon, mesocarbon microbeads, etc.) [49–52], the nitrogen-doped anode [53,54], the silicon-based anode (amorphous silicon, SiB_4, artificial graphite, etc.) [55–57], the tin-based anode (tin oxide, tin compound, etc.) [58,59], and the alloy anode (tin-based alloy, silicon-based alloy, bismuth-based alloy, etc.) [60–62], etc.

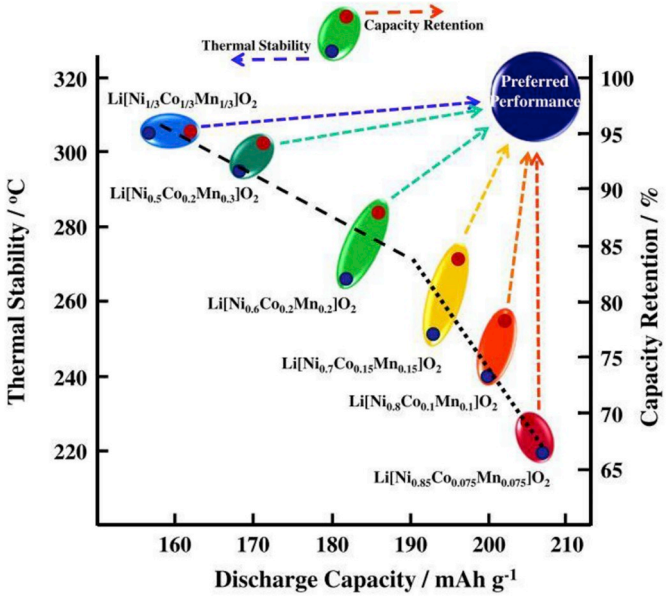

Fig. 2. A map of relationship between discharge capacity, and thermal stability and capacity retention of $Li/Li[Ni_xCo_yMn_z]O_2$ (x = 1/3, 0.5, 0.6, 0.7, 0.8 and 0.85) [37].

2.3. Electrolyte

The electrolyte is the only transmission channel inside a lithium-ion battery for the migration of lithium-ions and realize current conduction, and it is generally composed of the lithium salt, the organic solvent, and other additives. As an important component of the electrolyte, the lithium salt can provide free lithium ions and transport them inside a battery. Meanwhile, the lithium salt can form a protective layer on the surface of the electrode, which largely determines the capacity, the operating temperature, the cycle performance, the power density, the energy density, and the safety of lithium-ion batteries. At present, the lithium salt for a lithium-ion battery mainly includes the inorganic lithium salt (such as $LiPF_6$, $LiClO_4$, $LiBF_4$, $LiAsF_6$) and the organic lithium salt (Such as $LiC_4F_9SO_2$, $LiF_2S_2NO_4$, $(CF_3SO_2)_2NLi$).

The organic solvent is required to have a strong chemical stability and a wide electrochemical window during the operation of lithium-ion batteries, and not to react with the active substances of the cathode and anode, which otherwise would reduce the effect of lithium ions in polarization.

The organic solvents of lithium-ion batteries are mainly mixed by dimethyl carbonate (DMC), diethyl carbonate (DEC), ethyl methyl carbonate (EMC), ethylene carbonate (EC), and propylene carbonate (PC), etc. in different proportions. In addition, the additive is an organic matter added to improve the electrochemical performance of the electrolyte. Generally, it does not participate in the electrode reaction, but it rather changes the electrochemical performance of the electrolyte system and affects the migration condition of lithium ions, thereby boosting the charging/discharging capacity and the safety of lithiumion batteries

[63–65]. The electrolyte additive mainly includes the flame-retardant additive (dimethyl phosphate, trimethyl phosphate, etc.), the anti-overcharge additive (diphenylamine, polytriphenylamine, etc.), and the high voltage resistant additive (1,4-dicyanobutane, 1,3-dicyanopropane, sulfone, etc.) [66,67], etc.

2.4. Separator

The separator, which is a porous film in a lithium-ion battery that prevents active substances of the cathode and anode from directly reacting in the electrolyte [68], is usually made up of the polyethylene (PE) or the polypropylene (PP). The quality of which directly affects the nominal capacity, the calendar life, and the temperature resistance of lithium-ion batteries. The current-interruption temperature is an important index for evaluating the temperature resistance of the separator, which refers to the temperature when the separator melts, micropores of the porous film closed, and the internal impedance of the battery increases rapidly. If the current-interruption temperature is too high, the risk of overheating the battery increases. On the contrary, if the current interruption-temperature is too low, the capacity of lithium-ion battery attenuates. To avoid the aforementioned problems, the separator can be improved by coating the high-temperature ceramic on top of its surface [69].

2.5. Current collector

Both the copper foil and the aluminum foil are preferred as collector materials for lithium-ion batteries, since they are relatively inexpensive but come with good electrical conductivity and ductility. Specifically, the aluminum foil is often chosen as the current collector at the cathode side, since the potential of the cathode in a lithium-ion battery is higher than that of the anode. In addition, the high oxidation potential of the aluminum foil would make it more difficult to lose electrons or to be oxidized. Moreover, a passivating alumina layer will be formed on the surface of the aluminum foil after oxidation, which can further improve the oxidation resistance of the aluminum foil. Consequently, the copper foil with a lower oxidation potential is often used as the anode collector.

One major theme for the continuous development of lithium-ion battery technologies in recent years is the relentless pursuit of higher energy densities for all applications, from portable electronic devices to electric vehicles. To achieve this goal, the primary solution for the current collector is to reduce its thickness and weight. With the improvement of the preparation process of the copper foil and the aluminum foil, the thickness of the cathode aluminum foil has been reduced from 16 μm to 8 μm, and the thickness of the anode copper foil has been reduced from the previous 12 μm to 10 μm, and then to 8 μm, and nowadays there are manufacturers that can produce copper foils down to 6 μm.

In addition to its thickness and weight, the surface property of the current collector can also greatly affect the performance of lithium-ion batteries. Especially for the anode current collector, any preparation defects would bring asymmetry to both sides of the copper foil, which can further lead to asymmetries on the coating and the anode contact resistance, resulting in the inhomogeneous capacity on two sides of the anode electrode. Meanwhile, this asymmetry also causes inconsistency to the adhesion strength on the anode coating, which makes the cycle life of the anode's two sides become seriously unbalanced, thereby accelerating the degradation of the battery capacity.

2.6. Working principles

According to the migration model proposed by Padhi [70], when a lithium-ion battery is charged and discharged in the normal way, the insertion and extraction process of lithium ions are carried out from the surface of $LiMeO_2$ (Me stands for the transition metal, such as nickel) through a $LiMeO_2/Li_{1-x}MeO_2$ interface. This charging/discharging behavior will only change the crystal lattice distance among active substances, but it will not destroy the crystal structure. However, if a lithium-ion battery is overcharged or deeply discharged, the lattice can be distorted and the battery performance will suffer.

During a charging cycle, lithium ions are free from the lattice of the cathode, then they are injected into the electrolyte through the $LiMeO_2/Li_{1-x}MeO_2$ interface. Meanwhile, electrons are obtained from an external power supply, and they will flow into the cathode through the aluminum collector. In addition, free lithium ions are then embedded into the layered lattice of the anode's active substances. As the number of electrons flowing into the cathode increases (or the number of lithium ions embedded into the layered lattice increases), the energy of the lithium-ion battery increases. Conversely, during discharging, lithium ions are extracted from the layered lattice of the anode's active substances, then they are injected into the electrolyte and release electrons, the extracted lithium ions are then inserted into the crystal of the cathode's active substances through the electrolyte and separator. The released electrons can form a current conduction path in the external loop through a wire, and the lithium-ion battery begins to discharge and power a load.

2.7. Thermal runaway mechanism

Although the lithium-ion battery has a very high coulombic efficiency, the extraction and insertion of lithium ions between the two electrodes are not 100% energy-efficient, due to many factors such as the ohmic resistance, the polarization resistance, and the electrochemical reaction, etc. This imperfection in efficiency can make lithium-ion batteries generate additional heat in the normal condition, and even excessive heat under the impact of a mechanical abuse, an electrical abuse, or a thermal abuse. To make it worse, if the cooling methodology had underperformed in a lithium-ion battery system, additional heat can accumulate and lead to the rise of thermal runaway. Thermal runaway of lithium-ion batteries generally refers to the phenomenon of exothermic chain reactions inside batteries due to many electrochemical side reactions, causing a sharp temperature rise, damaging the battery's inner structure, and seriously degrading its performance [18].

The main cause of a thermal runaway event is the internal short-circuit fault, which can cause the temperature of lithium-ion batteries to go beyond control in a few minutes. When a lithium-ion battery suffers from a mechanical abuse caused by nail penetrations, crushing into an object, and dropping to the ground, etc., the separator can be teared down. When a lithium-ion battery suffers from an electrical abuse caused by overcharging, overdischarging, and external short-circuit, etc., the separator can be pierced. When a lithium-ion battery suffers from a thermal abuse caused by overheating, fire, high ambient temperature, etc., the separator collapses. Therefore, no matter how the separator is damaged, an internal short-circuit will occur in a lithium-ion battery, generating excessive heat and intensifying the degree of electrochemical side reactions. These unfavorable reactions can release a large amount of flammable gas, leading to an increased internal pressure and an expansion of the outer case of lithium-ion batteries, which can eventually develop into a fire or an explosion [71–73]. A schematic diagram of the thermal runaway process of lithium-ion batteries under various sources of abuse is illustrated in Fig. 3.

3. Heat generation and gas venting behavior of lithium-ion batteries

The temperature of lithium-ion batteries can rise due to the migration of lithium-ions and the electrochemical reaction, and in general this temperature rise will not adversely affect the performance and the safety of lithium-ion batteries at normal conditions. However, if there is an abuse that induces additional heat in the battery, the internal electrochemical side reaction can be intensified, generating a large amount of heat with flammable gases and eventually leading to a thermal runaway event. This section will summarize the heat generation mechanism and

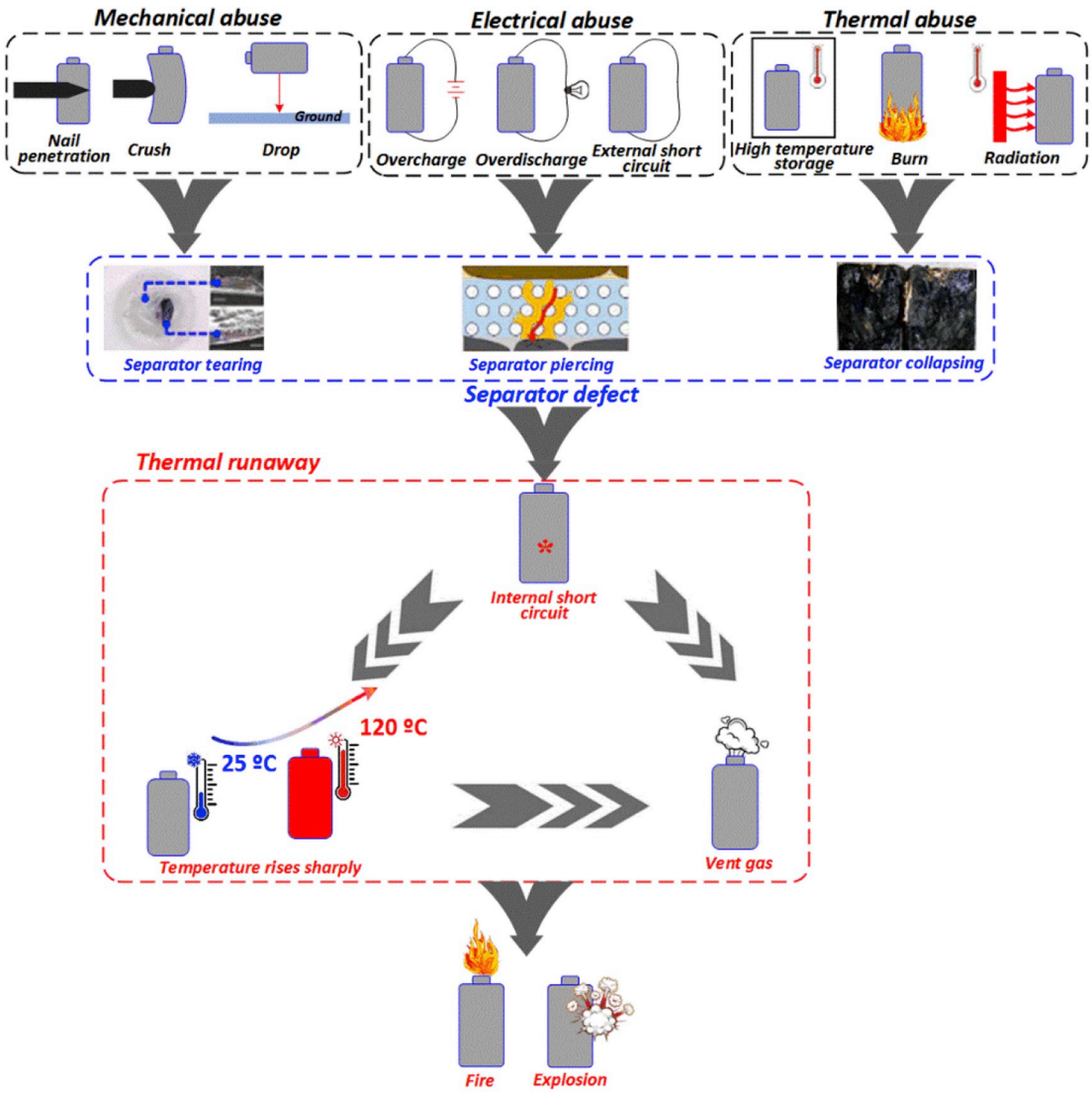

Fig. 3. Schematic diagram of the thermal runaway mechanism of lithium-ion batteries under various sources of abuse.

the gas venting behavior of lithium-ion batteries during the thermal runaway process.

3.1. Heat generation mechanism

The heat of lithium-ion batteries is mainly generated from the activation polarization loss (electrochemical reaction heat generated by interface charge transfer), the concentration polarization loss (overpotential heat generated by mass transfer), and the ohmic polarization loss (Joule heat generated by the motion of charged particles). The heat generation rate of a lithium-ion battery refers to the heat generated per unit volume per unit time. Under the normal charging and discharging condition, the Bernardi equation based on the law of conservation of energy is widely used in the study of heat generation characteristics of lithium-ion batteries [25].

The heating effect of electrochemical reactions was first proposed by Sherfey in 1958 [74]. In Sherfey's work, it is considered that the heat generation rate of the electrochemical reaction is determined by the current fraction, the entropy change, and the overpotential in each reaction. Subsequently, Gross [75] and Gibbard [76] evaluated the heat generation mechanisms and thermal properties of sealed batteries based on the heating effect of electrochemical reactions. Remarkable contributions regarding the heat generation model of lithium-ion batteries were not made until 1985 when Bernardi et al. proposed a thermodynamic energy conservation equation, which is later referred to as the Bernardi equation. The Bernardi equation is mainly composed of heat generated from the reversible and the irreversible reactions. While the heat of the reversible reaction is caused by the electrochemical reaction, the heat of the irreversible reaction includes the Joule heat generated by the ohmic polarization, the electrochemical heat generated by the activation polarization, and the overpotential heat generated by the concentration polarization [77]. The Bernardi equation for lithium-ion battery heat generation is given below as

$$Q = q_{rev} + q_{irev} \tag{1}$$

$$q_{rev} = -\frac{J/2}{d_{ca} + d_s + d_{an}} T \frac{\partial U_{oc}}{\partial T} \tag{2}$$

$$q_{irev} = \frac{J^2 R/2}{d_{ca} + d_s + d_{an}} \tag{3}$$

where q_{rev} and q_{irev} are the heat generation rate of the reversible and the irreversible reactions, respectively, $\partial U_{oc}/\partial T$ is the entropy heat coefficient, d_{ca}, d_s, d_{an} are thicknesses of the cathode electrode, the separator, and the anode electrode, respectively.

In addition, during a lithium-ion battery thermal runaway process, a

series of uncontrollable electrochemical side reactions can occur in the active substances of the cathode, the anode, the electrolyte, and the separator of lithium-ion batteries. A large amount of heat would be generated through substance decomposition, thus the equation of heat generation rate for a lithium-ion battery undergoing a thermal runaway process is

$$Q = q_{rev} + q_{irev} + q_{de} \tag{4}$$

where q_{de} is the heat generation rate from substance decomposition during thermal runaway.

Based on heat generation models of the cathode and anode proposed by Hatchard et al. [78] for lithium-ion batteries during high-temperature-induced thermal runaway, Huang et al. [79] combined both models with the Semenov model (assuming the temperature distribution inside the electrochemical reactants is uniform) and the Thomas model (assuming the temperature distribution inside the electrochemical reactants is non-uniform), and then used the exothermic reaction in the thermal runaway process as a weighting factor to establish a thermal abuse correction model with heat generation equations.

According to the model proposed by Hatchard, the total heat generation rate of electrochemical side reactions during the thermal runaway process is approximately the Arrhenius equation as follows [78].

$$q_{de} = V\Delta Hc^{n}Aexp(-E_a/RT) \tag{5}$$

where V is the volume of component substances of a lithium-ion battery, ΔH is the heat generated by electrochemical side reactions, c is the reactant's concentration involved in electrochemical side reactions, n is the reaction order, E_a is the activation energy, R is the universal gas constant, and T is the reaction temperature. On the basis of the law of conservation of energy, the heat generation equation of a lithium-ion battery during thermal runaway induced by the thermal abuse is

$$\rho C_p\frac{\partial T}{\partial t} = k\left(\frac{\partial^2 T}{\partial x^2} + \frac{j}{x}\frac{\partial T}{\partial x}\right) + V\Delta Hc^{n}Aexp\left(-\frac{E_a}{RT}\right) \tag{6}$$

where ρ is the density of the lithium-ion battery, C_p is the specific heat capacity, k is the thermal conductivity, j is the form factor ($j = 0$ indicates an infinity plate, $j = 1$ indicates an infinite cylinder, and $j = 2$ indicates a sphere).

Moreover, Yamanaka et al. [11] established a heat generation model of lithium-ion batteries during thermal runaway based on a nail penetration abuse and substance decomposition reactions. The density of the generated Joule heat during the nail penetration is

$$Q_{nail} = \frac{d}{\sigma_{nail}S}\left(\frac{\varphi_p - \varphi_n}{R_c + d/\sigma_{nail}S}\right)^2 \Big/ V_{nail} \tag{7}$$

where d is the total depth of nail piercing, σ_{nail} is the electrical conductivity of the nail, S is its cross-sectional area, so the nail resistance is $R_{nail} = d/\sigma_{nail}S$, φ_p and φ_n are the average electrical potentials of the cathode collector/nail and the anode collector/nail interfaces, respectively, R_c is an adjustment parameter of internal short-circuit resistance ($R_{sc} = R_{nail} + R_c$) during thermal runaway caused by nail penetration.

3.2. Gas venting behavior

When lithium-ion batteries are subject to abuses from various sources, they can develop into thermal runaway processes that mainly incorporate the following steps: the solid-electrolyte interphase (SEI) decomposes, the anode collapses, the intercalated lithium reacts with the electrolyte, the separator melts, the cathode's active substances and the electrolyte lithium salt decompose, the electrolyte solvent oxidizes, the intercalated lithium reacts with the binder, the ceramic coating of separator collapses, and the internal short-circuit occurs. During these periods, not only does the temperature of a lithium-ion battery change abruptly, a fair amount of gas is also released [80,81].

During SEI decomposition, the temperature of lithium-ion batteries can reach up to 80 to 120 °C, and the meta-stable substance in the SEI will decompose and produce CO_2, O_2, and some flammable hydrocarbon. Being a strong oxidizing gas, O_2 will aggravate the degree of electrochemical side reactions inside the lithium-ion batteries. In addition, O_2 is also a combustion adjuvant, which further threatens the safety of lithium-ion batteries. Taking the meta-stable materials $ROCO_2Li$ and $(CH_2OCO_2Li)_2$ as examples, the decomposition reactions are [82–84]

$$ROCO_2Li \rightarrow ROLi + CO_2\uparrow \tag{8}$$

$$(CH_2OCO_2Li)_2 \rightarrow Li_2CO_3 + C_2H_4\uparrow + CO_2\uparrow + \frac{1}{2}O_2\uparrow \tag{9}$$

wherein R is among the alkyl group, such as $–CH_3$, $–C_2H_5$.

After the anode collapses, the intercalated lithium inside the anode will be directly exposed to the electrolyte and undergoes an exothermic reaction, producing flammable hydrocarbon. Taking EC, DMC, PC, and DEC as examples, these exothermic reactions are [85]

$$C_3H_4O_3(EC) + 2Li \rightarrow Li_2CO_3 + C_2H_4\uparrow \tag{10}$$

$$C_3H_6O_3(DMC) + 2Li \rightarrow Li_2CO_3 + C_2H_6\uparrow \tag{11}$$

$$C_4H_6O_3(PC) + 2Li \rightarrow Li_2CO_3 + C_3H_6\uparrow \tag{12}$$

$$C_5H_{10}O_3(DEC) + 2Li \rightarrow Li_2CO_3 + C_2H_4\uparrow + C_2H_6\uparrow \tag{13}$$

As the intensity and degree of electrochemical side reaction increase, the separator melts, the active substances of the cathode decompose, and the electrolyte lithium salt begins to decompose and produce toxic and flammable gases. Taking a typical type of lithium-ion battery as an example in which the active substances of the cathode is $Li_xMn_2O_4$, and the electrolyte lithium salt is $LiPF_6$, then the oxygen-evolving reaction of $Li_xMn_2O_4$ and the decomposition reaction of $LiPF_6$ are shown below as [12,86–88]

$$Li_xMn_2O_4 \rightarrow xLiMnO_2 + \frac{x}{3}Mn_3O_4 + (1-x)Mn_2O_3 + \frac{3-x}{6}O_2\uparrow \tag{14}$$

$$LiPF_6 \rightleftharpoons LiF + PF_5 \tag{15}$$

Subsequently, the organic electrolyte solvent is oxidized, and the oxygen is produced by the SEI decomposition reaction and the cathode oxygen-evolving reaction, which further leads to an abrupt increase of the heat generation rate inside lithium-ion batteries, as well as the release of a large amount of gas mixtures and vapors. Taking the organic electrolyte solvent EC and DEC as examples,

$$4C_3H_4O_3(EC) + 7O_2 \rightarrow 6CO\uparrow + 6CO_2\uparrow + 8H_2O\uparrow \tag{16}$$

$$4C_3H_6O_3(DEC) + 9O_2 \rightarrow 6CO\uparrow + 6CO_2\uparrow + 12H_2O\uparrow \tag{17}$$

Meanwhile, PF_5, one of the products of the $LiPF_6$ decomposition reaction, can react with vapor to form the hydrogen fluoride (HF) and the phosphorus oxyfluoride (POF_3), which are harmful to human beings. In addition, it can also react with Li_2CO_3, a stable substance of the SEI, to produce the greenhouse gas. Moreover, HF can react with Li^+ in the electrolyte to form LiF and hydrogen radicals. A large number of hydrogen radicals combined can form hydrogen that is prone to explosion, adding another safety concern to the lithium-ion battery [21,89].

For the binder polyvinylidene fluoride (PVDF), which is used to bond and maintain the active substances of the cathode and anode, can react with the intercalated lithium metal of the cathode or anode at high temperatures, producing some flammable and explosive gases as [90]

$$[\,CH_2 - CF_2\,]_n + Li \rightarrow [\,CH_2 = CF_2\,]_n + LiF + \frac{1}{2}H_2\uparrow \quad (18)$$

Finally, the electrolyte solvent vapor in lithium-ion batteries and the flammable gases generated by the decomposition reactions are concentrated, causing the battery case to rupture and prone to ignition due to electric arcs (generated by the external circuit) or sparks (generated by the friction of the high-speed particles and the battery case).

In order to analyze the degradation mechanism of lithium-ion batteries during thermal runaway [91], Fernandes et al. [92] performed a pyrolysis experiment on the DEC and EMC in inert gas, and they found that the DEC degradation would produce carbon dioxide, dimethyl ether, carbon monoxide, hydrogen, and hydrocarbon at 300 °C, while EMC degradation can produce carbon dioxide, dimethyl carbonate, diethyl carbonate, and hydrocarbon. This experiment indicates that the electrolyte solvent mainly undergoes the transesterification reaction and the thermal decomposition reaction at 300 °C. Fernandes' experiment also shows that the gas composition and total gas emissions during the thermal runaway process of lithium-ion batteries are related to the severity of an abuse.

In 2018, Fernandes et al. [93] performed a review on the venting behavior of lithium-ion batteries during thermal runaway caused by an electric abuse involving overcharging, overdicharging, and overheating. Furthermore, Koch et al. [94] carried out an experiment, in which 51 different fully-charged lithium-ion batteries (including the pouch and hard case) were heated separately by a home-made sealed kettle to trigger the thermal runaway process. Finally, the total amount and the composition of gases released during thermal runaway were measured and analyzed, and it is found that the total amount of venting gas is linearly related to the capacity of the lithium-ion battery, with an approximate formula of V_{vent} (L) = 1.961 × C_{cell} (Ah).

4. Thermal runaway monitoring and detection methods for lithium-ion batteries

For the majority of applications employing lithium-ion batteries, such as the energy storage component of micro-grids and the battery pack of electric vehicles, are actually using modules composed of a large number of lithium-ion battery cells connected in series and in parallel, all stacked in a specific container. If one or a few lithium-ion battery cells in the container experienced thermal runaway, due to the extremely constrained container space and the heat transfer among battery cells through convection and conduction, some local heated spots will be created, which further leads to the propagation of thermal runaway failures to all of the neighboring cells. Due to the domino effect, all of the lithium-ion battery cells in the container can ultimately run into thermal runaway failures [95–99].

Based on the mechanism of thermal runaway, it is applicable and convenient to take the voltage/current, the temperature, and the released gas as the characteristic fault signals to monitor and detect the presence of thermal runaway events in lithium-ion batteries. This section will discuss and summarize three types of thermal runaway monitoring and detection schemes as follows:

1) Real-time detection of the lithium-ion battery cell/module terminal voltage and its surface temperature;
2) Real-time monitoring and estimation of the internal temperature and the strain of lithium-ion batteries;
3) Real-time monitoring and analyzing the characteristic vent gas component of lithium-ion batteries during thermal runaway.

4.1. Terminal voltage and surface temperature monitoring methods

The battery management system (BMS) is the most widely used method for monitoring and detecting thermal runaway events in lithium-ion battery applications. It mainly relies on the built-in voltage sensors and temperature sensors as measurement tools. With a sufficient number of sensors installed, this system can measure the terminal voltage and the surface temperature of each lithium-ion battery cell in real time. Once an abnormal signal is detected, the BMS can trigger an alarm immediately [100–102].

In addition, in order to accurately detect the terminal voltage of each lithium-ion battery cell, a multi-voltage sensor based interleaving voltage topology measurement scheme is proposed by Xia et al. in [103]. This method designs the voltage sensor topology for lithium-ion batteries with redundancy, and then it applies an intelligent algorithm, a control circuit, and an accurate voltage threshold to monitor the presence of a voltage anomaly for each lithium-ion battery cell in a series-connected battery pack. If a lithium-ion battery cell experienced thermal runaway caused by overcharging or overdischarging, the corresponding voltage sensor value would change, i.e., if the voltage sensor value is lower than the minimum threshold, a lithium-ion battery cell is considered to be overdischarged, else it is considered to be overcharged [103–105].

The topology of the thermal runaway monitoring and detection method based on multiple voltage sensors is shown in Fig. 4. The prevailing voltage measurement method applies a voltage sensor across each lithium-ion battery cell, as shown in Fig. 4(a). While in real applications, voltage sensors have their own reliability issues, and thus a sensor fault may trigger a false alarm for the battery failure. In many industry applications, therefore, a second sensor for each battery cell will be added to provide redundancy. In this way, the data from the second-layer sensor will provide a cross-validation to the first-layer sensor, as Fig. 4(b) shows its embodiment applied to a series-connected battery pack. This two-layer sensor hierarchy can detect a battery fault when both sensors give consistent outputs. When two sensors corresponding to the same battery cell have different readings, it is very likely that a sensor fault occurs. However, despite offering a good level of accuracy and redundancy, this method also doubles the amount of sensors, as well as the cost related to the sensor and the wiring harness.

One common solution to this problem is to only add a redundant sensor to a string of battery cells rather than each individual cell, as shown in Fig. 4(c), in which only one redundant voltage sensor V6 is added in addition to an individual voltage sensor for each individual cell. This method can improve the accuracy of the battery failure detection to some extent, however, it is still not able to distinguish a sensor failure from a battery cell failure when sensor readings are inconsistent. Another voltage measurement topology is illustrated in Fig. 4(d), which measures an accurate reference voltage from an integrated chip during each sampling period. This reference voltage can be used to calibrate the sensor gain/offset and distinguish a sensor calibration error from a sensor hardware error. However, this method requires a precise voltage reference for each of the voltage measurement circuit, and it also increases the time consumed for taking each voltage measurement by one clock cycle, which is the time required to update the reference voltage during each sampling period.

Besides, this method will incorrectly attribute a switch malfunction to a battery fault. One solution to this problem is to adopt a fault-tolerant voltage measurement method, as shown in Fig. 4(e), in which each voltage sensor measures the voltage sum of two batteries. For example, the voltage of battery cell C2 is included in the measurements of both V1 and V2 sensors. The terminal voltage of C2 will drop when it is in an external short-circuit condition or is experiencing a thermal runaway event, and this abnormal voltage can be revealed by both V1 and V2 sensors as their readings will drop significantly below 6 V. On the other hand, when a sensor fault occurs, it can be immediately identified and distinguished from a battery/switch fault, since it is impossible for only one sensor reading to change. For example, if at a time instant, readings of sensors V1 to V4 are all 6 V, while only V5 significantly deviates from

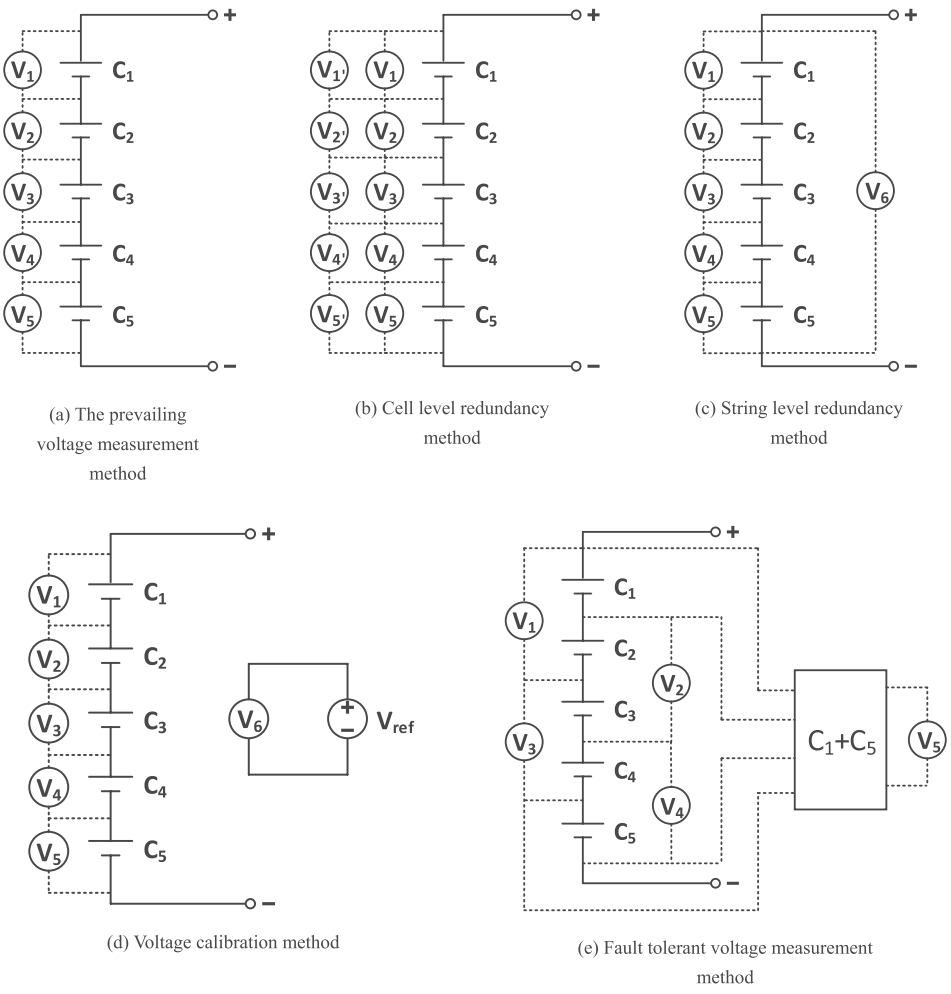

Fig. 4. Schematics of thermal runaway monitoring and detecting method based on muti-voltage sensors.

6 V, it would be almost certain that sensor V5 is experiencing a hardware failure or a bad connection.

Another advantage of the voltage sensor-based approach is the ability to locate a faulty battery cell inside a battery pack, which is hard to accomplish for the temperature or gas component-based monitoring methods. However, the multi-sensor method can be costly because of the large number of voltage sensors required. In addition, a large amount of sensing data also poses a great computation burden to the digital signal processor in the BMS. For example, a large lithium-ion battery system is typically composed of thousands of batteries, such as an electric vehicle battery pack. If a voltage sensor is applied across each battery cell, a large amount of sensor data will be transmitted to the BMS. This amount of real-time data would potentially occupy much of the BMS processing resource and storage, thus threatening the capability and robustness of the BMS to effectively regulate the charging/discharging behaviors.

Therefore, a common practice in industry is to only install a voltage sensor to be shared by many battery cells instead of each individual cell. For example, the luxury version of the Tesla Model S battery pack has 14 modules connected in series, while each module has 6 cells in series and 74 cells in parallel, giving a total of 7,104 cells in the entire battery pack. However, since all of the parallel-connected cells would share one voltage sensor, only $6 \times 14 = 84$ out of a total of 7,104 voltage sensors are needed. Besides cell voltages, temperatures of the positive and the negative module terminals are also measured by a Battery Monitoring Board (BMB) mounted on one end of each module. A 10-pin Molex connector at the top of this BMB allows connection to a daisy chain cable assembly connecting all of the modules to a central BMS board at the end of the main battery assembly, which then communicates with other vehicle components via the Controller Area Network (CAN) bus [106].

Regarding to the methods used for monitoring and detecting the surface temperature of a lithium-ion battery pack, the temperature sensor is usually a thermistor or a thermocouple. However, both types of temperature sensors have similar problems such as the low detection accuracy and the vulnerability to environment change. In order to improve the detection accuracy of surface temperature and improve the reliability for monitoring and detecting a thermal runaway process with the surface temperature data, Nascimento et al. [107] employed fiber Bragg grating optical sensors and K-type thermocouples to detect the surface temperature at the top, middle, and bottom part of the lithium-ion battery at both the normal and abnormal state with various discharge rates (0.53 C, 2.67 C, and 8.25 C). Locations of fiber Bragg grating optical sensors and K-type thermocouples are illustrated in Fig. 5 (a). It is found that the fiber Bragg grating optical sensor has a better temperature resolution and a higher temperature sensitivity when compared to a K-type thermocouple. The result from [107] also indicates that the fiber Bragg grating optical sensor can be used to detect the surface temperature of lithium-ion batteries in real-time, thus improving the performance and robustness for monitoring and detecting the thermal runaway process of lithium-ion batteries with BMS.

Thereafter, based on the fiber Bragg grating optical sensor, the same team proposed a fiber optical sensor network for measuring the surface temperature of lithium-ion batteries. Through experimentation, the surface temperature of a lithium-ion battery in a smartphone was detected in real-time, both *in-situ* and *in operando* with multi-point

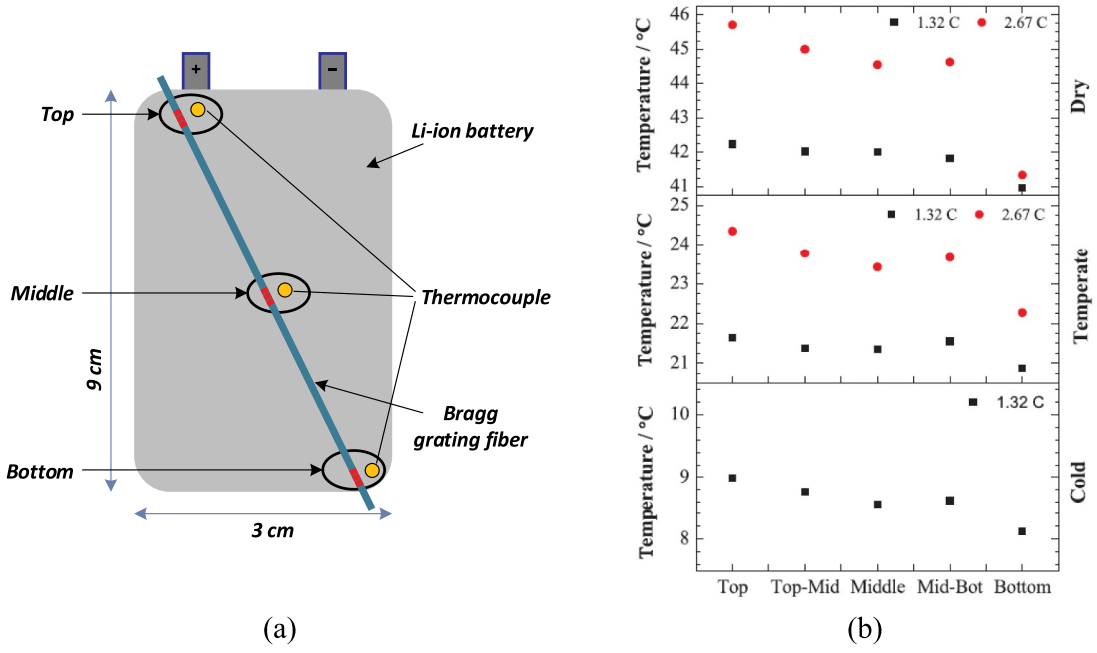

Fig. 5. Thermal runaway monitoring and detecting method based on surface temperature measurement: (a) the location of fiber Bragg grating optical sensor and K-type thermocouple [107]; and (b) the absolute surface temperature of each position [108].

monitoring at various discharge rates in a dry environment [108]. It is found that the surface temperature of a lithium-ion battery in a smartphone during the thermal runaway process induced by a large discharge rate is nearly twice as much as the temperature at normal conditions. In addition, the fiber Bragg grating optical sensor is used to detect the absolute surface temperature that is discharged at 5.77 C, and its surface temperature is as high as 65 °C. There is also an obvious tendency of temperature decrease from the top to the bottom of the battery cell, with the temperature of each position shown in Fig. 5(b). The highest temperature detected is at the top of the battery cell (close to the electrodes), followed by the top-middle position. The temperature at the mid-bottom is slightly higher than that of the middle, and the temperature detected at the bottom of the lithium-ion battery is the lowest among all of the above positions.

4.2. Internal state monitoring methods

For a fully enclosed lithium-ion battery, however, it is almost impossible to thoroughly and accurately monitor its health condition by simply monitoring the terminal voltage and the surface temperature. In this case, the internal temperature should be used as the characteristic fault signal. In order to investigate the correlation between the internal temperature and the surface temperature of a lithium-ion battery, Grandjean et al. [109] conducted a thermal characteristic numerical simulation based on a lithium-ion battery with a large discharge rate, and it is observed that the difference between the internal temperature and the surface temperature can be as much as 20 °C. In addition, Parhizi et al. [110] established an internal temperature tracking model based on the thermal conductivity analysis during the thermal runaway process. The experiment tested two 18650 cylindrical lithium-ion batteries composed of $LiNi_{0.45}Co_{0.1}Mn_{0.45}O_2$ and $LiMn_2O_4$ to validate the reliability of the internal temperature tracking model via experiments. It is found that the maximum internal core temperature is nearly 500 °C higher than the surface temperature of the lithium-ion battery during thermal runaway.

Specifically, some of the most widely used internal state monitoring methods for lithium-ion batteries are based on the embedded fiber sensors and the electrochemical impedance spectroscopy (EIS) analysis [111].

4.2.1. Embedded fiber sensors

In order to accurately monitor the internal core temperature of lithium-ion batteries, Du et al. [112] proposed a method for predicting the internal core temperature of lithium-ion batteries based on the fluorescence lifetime measurement, and they implemented an apparatus based on this method with a nickel-coated fluorescent fiber. This apparatus mainly consists of a fluorescent excitation source with a wavelength of 470 nm, a source driving circuit, an optical coupling system, a fluorescent signal detection and processing system, and a display system. To start with, a nickel-coated fluorescent probe is buried inside the battery core. The schematic of the apparatus implemented by Du is shown in Fig. 6(a). When the rare-earth material on the fluorescent probe is exposed to an ultraviolet source, it will excite the fluorescence and emit the afterglow, and the decay lifetime of the afterglow is a single-valued function of temperature, that is, the higher the temperature, the shorter the decay lifetime.

Similarly, Raghavan et al. [113–115] implemented an internal state monitoring apparatus based on the embedded fiber Bragg grating optical sensor, whose refractive index and refracted wavelength are both subject to change with the battery's internal strain and temperature. Therefore, by measuring the change of the refracted wavelength, the strain and temperature inside a lithium-ion battery can be estimated. The embedding position and the fiber Bragg grating optical sensor coated with corrosion-resistant material are essential to the success of this internal state monitoring apparatus. During implementation, the sensing gate area of the Bragg fiber is pasted on the lithium-ion battery's electrode, and then the Bragg fiber is attached with fireproof adhesive tapes. It must be noted that the fiber should be kept away from the lithium-ion battery cores and lugs, and be subsequently packaged. An illustrative diagram with embedding positions of the Bragg fiber is shown in Fig. 6(b).

The fiber Bragg grating optical sensor can directly monitor and detect the internal strain and temperature change of lithium-ion batteries. However, due to this capability to detect both signals simultaneously, Nascimento et al. [116] found that the single Bragg fiber-based monitoring method can be defective since the two signals can actually

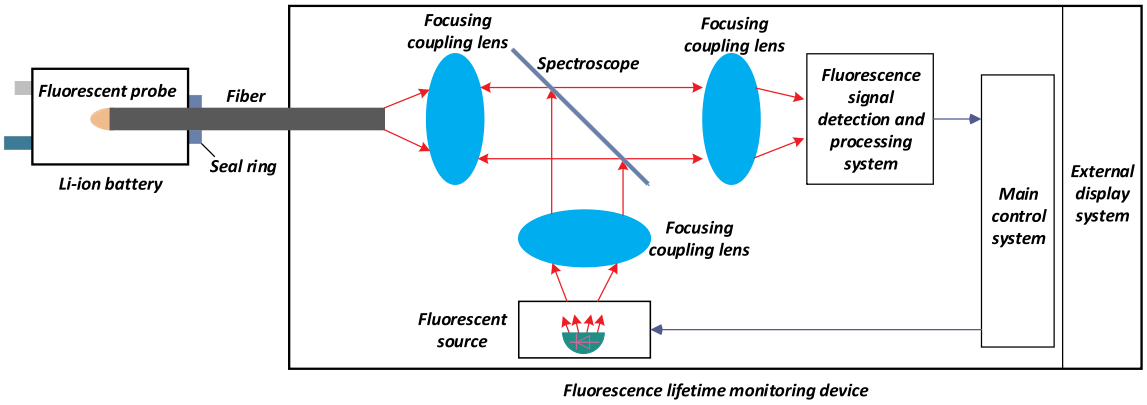

(a) Fluorescence lifetime sensor method [112].

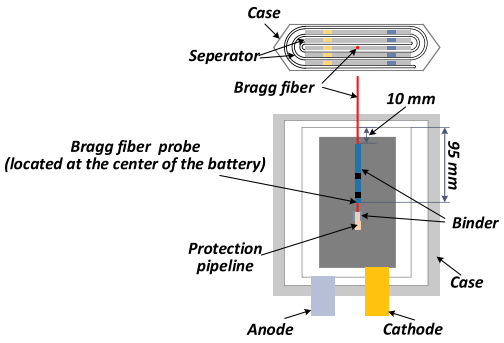

(b) Embedded Bragg fiber optic grating sensor method [113].

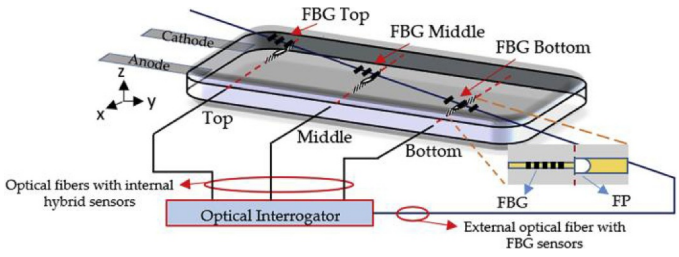

(c) Bragg fiber-Fabry-Perot hybrid sensors method [116].

Fig. 6. Schematics of internal temperature monitoring methods of lithium-ion batteries based on various sensors.

interfere with each other, which makes it impossible to quickly and accurately identify the internal temperature of lithium-ion batteries during thermal runaway. Therefore, based on the fact that the Fabry-Perot is extremely strain-sensitive but temperature-insensitive, Nascimento et al. [116] proposed an internal temperature detecting method for the lithium-ion battery by coupling the fiber Bragg grating with the Fabry-Perot, and then subtract the internal strain signal detected by the Fabry-Perot from signals detect by the fiber Bragg grating to obtain an accurate internal temperature of the lithium-ion battery. The schematic diagram of this internal temperature monitoring method based on the Bragg fiber-Fabry-Perot hybrid sensor is shown in Fig. 6(c).

4.2.2. Electrochemical impedance spectroscopy (EIS) analysis method

The electrochemical impedance spectroscopy (EIS) is a popular non-destructive technique used to characterize the electrochemical behavior of lithium-ion batteries. Both the impedance phase shift and the amplitude can be used to monitor and detect the internal temperature of lithium-ion batteries.

The correlation between the battery's internal temperature and thermal runaway is further illustrated in [117], which states the impedance response correlates to the anode/SEI layer. Since SEI is reported to be thermally stable up to around 100 °C, decomposition may occur above this temperature, leading to the deactivation and/or total failure of a battery. It is therefore of great importance to be able to track the internal battery temperature up to this critical point of 100 °C.

In [118,119], Raijmakers et al. analyzed the EIS of lithium-ion batteries with changes in the state of charge (SOC) and temperature, and they proposed a method to estimate the internal temperature of lithium-ion batteries based on the interception frequency f_0 of the electrochemical impedance, which is defined as the frequency when the voltage and current are in phase. The mechanism lies in the fact that this impedance interception frequency is only related to the internal temperature, but is unrelated to the SOC of lithium-ion batteries.

In addition, Srinivasan et al. [120,121] proposed a method for estimating the internal temperature of a lithium-ion battery based on the phase shift of the electrochemical impedance. Specifically, an electrochemical impedance meter (Solartron SI1287) and a frequency response analyzer (Solartron SI1250) are used together to detect the impedance phase shift (Φ) and amplitude (|Z|) of two different commercial lithium-ion batteries: a 53 Ah GS Yuasa lithium-ion battery and a 5.3 Ah Boston Power lithium-ion battery. It is observed that while the correlation between the impedance phase shift and the battery capacity is rather weak, there exists a strong relationship between the impedance phase shift and the internal temperature of the lithium-ion battery. Subsequently, the same team implemented an internal temperature monitoring and detection apparatus based on this impedance phase shift method by using a printed circuit board (PCB) integrated to the BMS to form a phase shift monitor [122]. The result showcased that an early warning of a thermal runaway event can be achieved in real-time by monitoring the impedance phase shift. Fig. 7(a) shows the strongly-correlated impedance phase shift versus the internal temperature of the two lithium-ion batteries under test, when the electrochemical impedance excitation frequency is 40 Hz. In addition, Fig. 7(b) illustrates the variation of the impedance phase shift and surface temperature of a lithium-ion battery during a thermal runaway process.

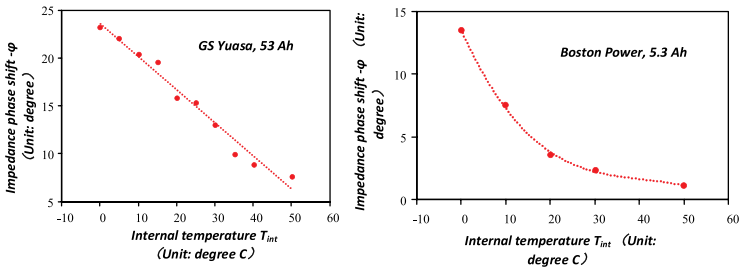

(a) Impedance phase shift v.s. internal temperature [120].

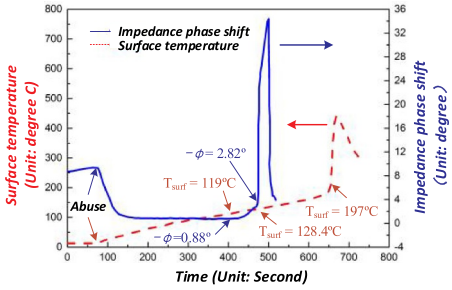

(b) Impedance phase shift v.s. surface temperature, revised from [120].

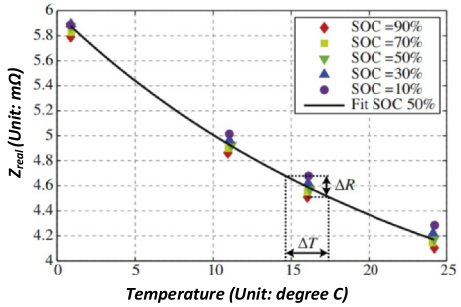

(c) Real part of the impedance at 10.3 kHz v.s. internal core temperature, shown in various SOC [124].

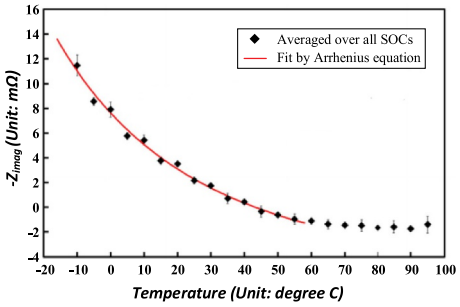

(d) Imaginary part of the impedance at 300 Hz v.s. internal core temperature, averaged over all SOCs [117].

Fig. 7. Internal temperature monitoring of lithium-ion batteries based on electrochemical impedance spectroscopy.

In Fig. 7(a), the impedance phase shift of the 53 Ah GS Yuasa lithium-ion battery is linearly related to the internal temperature, while the 5.3 Ah Boston Power lithium-ion battery curve is nonlinear. In Fig. 7(b), the surface temperature changes slowly at the initial stage of thermal runaway, while the impedance phase shift Φ drops and remains stable at a value close to 0. When the surface temperature T_{surf} reaches 119 °C, the battery shows no indication of venting gas, and it would take an additional 55 s for the battery to vent. When T_{surf} reaches 128 °C, however, Φ experiences a significant increase, from 0.8° to 35°, but the surface temperature is still rising slowly, indicating the impedance phase shift Φ is a much better indicator for monitoring the gas venting and the thermal runaway process when compared to the surface temperature T_{surf}. The vent gas mixture is presumably generated during the chemical reaction between the graphite anode and the electrolyte after the temperature reaches above 80 °C. The battery cell has vent valves, and as the pressure inside the battery increases due to gas generation, the vent valve will open and release the excessive gas, which would ultimately reduce the inner pressure and cool down the battery. Therefore, the observed large variations of Φ can be expected and may serve as a good indicator for the thermal runaway process.

Similarly, Schwarz et al. [123] estimated the internal core temperature of the titanate cathode lithium-ion battery by using the electrochemical impedance spectrum, which is generated by a 1 kHz square-wave excitation signal. An apparatus based on this approach is also implemented with a PCB prototype and integrated into the BMS. Finally, the result shows the internal core temperature of the lithium-ion battery can be effectively estimated in a real time manner.

Besides the impedance phase shift or magnitude varation, the real and imaginary part of the battery internal impedance can be also implemented to monitor the thermal runaway process [117,124]. For example, Schmidt et al. [124] analyzed the internal temperature of a commercial 2 Ah pouch battery using the EIS excited by a 10.3 kHz source, and a relationship between the real part of the electrochemical impedance and the internal core temperature is obtained, as shown in Fig. 7(c). It is observed that the relationship is similar to the Arrhenius equation adding a constant resistance [124], which is described in detail as follows.

The Arrhenius equation is an empirical formula for the relationship between the rate of chemical reactions and temperature, which can be written as

$$Z(f_m, T) = Ae^{E_a/RT} \tag{19}$$

where $Z(f_m, T)$ is the battery impedance, which is a function of the electrochemical excitation frequency f_m and the thermodynamic temperature T. In addition, A is the frequency factor, E_a is the activation energy, and R is the molar gas constant. As mentioned earlier, the relationship between the real part of the electrochemical impedance and the internal core temperature in Schmidt's article [124] is very similar to a revised Arrhenius equation as

$$Z(f_m, T) = Ae^{E_a/RT} + R_c \tag{20}$$

where R_c is the resistance of the metallic collector, and it is almost a constant within the investigated temperature range. It is identified in [124] that by adding this additional collector resistance term R_c on top of the original Arrhenius equation, the experimental curve in Fig. 7(c) can match this theoretical result very well, indicating that the real part of the electrochemical impedance can accurately reveal the internal temperature of a lithium-ion battery, which can be further used to monitor the thermal runaway process.

In regards to the imaginary part of the electrochemical impedance, Spinner et al. [117] monitored the instantaneous internal temperature

of a commercial 18650 $LiCoO_2$ lithium-ion battery by using the single-point EIS measurement, which is excited by a 300 Hz source. It is observed that the relationship between the imaginary part of the electrochemical impedance and the internal core temperature of lithium-ion batteries can be fitted by the conventional Arrhenius equation, as shown in Fig. 7(d). The close agreement between the experimental measurements averaged over all of the SOCs and the theoretical result obtained by the Arrhenius equation suggests that the variation of the battery inner impedance with respect to temperature has a highly predictable pattern based on its inner chemical reactions, as the Arrhenius equation can provide the theoretical ground for estimating the interior temperature of a battery using its internal impedance value.

In this same research conducted by Spinner et al. [117], the application of instantaneous single-point EIS measurements in monitoring the internal temperature of a lithium-ion battery above 95 °C is realized for the first time. This work is built upon the prior result from Srinivasan [120,121], Schmidt [124], and many others showing the internal temperature and the state of health of lithium-ion batteries can be monitored via the instantaneous, single-point impedance analysis. In these previous studies, temperatures greater than 65 °C have not been successfully tracked, limiting the potential to pinpoint the inter-phase decomposition of the solid-electrolyte above 100 °C or predict any impending battery failure. This work indicates that the internal temperature monitoring and detection method based on the EIS measurement is a promising tool for the next-generation lithium-ion battery thermal runaway diagnosis.

Furthermore, in order to provide the theoretical ground for the internal temperature monitoring and detecting method of lithium-ion batteries based on EIS measurements, Zhu et al. [125] decomposed the EIS into three parts: the ohmic resistance point, the kinetically controlled region, and the diffusion-controlled region. The ohmic resistance is derived from the solid electronic conduction and the lithium-ion transfer in the battery electrolyte. The kinetic impedance and the diffusion impedance are derived from the electrochemical charge transfer and the electric double-layer reaction, respectively. According to the established mechanism of the ohmic resistance, the kinetic impedance, and the diffusion impedance, an impedance spectra matrix analysis method is used to theoretically derive the magnitude variation and the phase shift of the electrochemical impedance, and an experiment is elaborated to explain how the impedance phase shifts and the its amplitude varies with respect to the internal temperature, the state of charge, and the state of health of lithium-ion batteries.

In summary, the internal temperature monitoring and detection method of a lithium-ion battery based on EIS can be performed by monitoring a number of impedance spectrum parameters such as the interception frequency, the phase shift, the real part, and the imaginary part of the battery impedance, etc. The key to accurately predicting the internal temperature and subsequently the thermal runaway of lithium-ion batteries lies in the proper selection of the excitation source, including the pattern and frequency of the excitation signal [126]. A critical point of internal temperature is around 100 °C for the anode/SEI layer to become vulnerable and prone to thermal runaway.

4.3. Venting gas detection methods

During the thermal runaway process, the BMS often times cannot detect this failure if it is still at the its incipient stage, since changes of characteristics signals such as the battery temperature, the discharge voltage, and the discharge current, etc. are not clearly visible. However, due to the electrochemical reaction inside the lithium-ion battery, a noticeable amount of gas will be produced even at this incipient stage, and thus monitoring and detecting thermal runaway events by using gas sensors could yield more sensitive and accurate early-stage diagnosis result [93,94]. This statement can be backed up by an experiment conducted by Koch et al. [127], who used a voltage sensor, a temperature sensor, a gas sensor, a smoke detector, a pressure sensor, and a creep distance sensor to monitor and detect the presence of a thermal runaway process of a lithium-ion battery module is thermally abused or mechanically abused with nail-penetration, as shown in Fig. 8(a). The result reveales that the gas sensor method is able to detect a thermal runaway event earlier than other sensor-based methods, no matter how such as abuse is induced [127].

In [128], Wang et al. implemented a thermal runaway automatic detection and warning apparatus based on Figaro gas sensors (TGS822TF). Specifically, this apparatus is mainly composed of a gas collecting device, a gas monitoring device, a control device, and an alarm device. The schematic diagram is illustrated in Fig. 8(b), where the Figaro gas sensor is highly sensitive to hydrogen and carbon monoxide, and its measurement range varies from 100 ppm to 1000 ppm (part per million) at room temperature. When the sensor detects the concentration of carbon monoxide or hydrogen exceeding 120 ppm, an alarm signal will be triggered.

Similar to [128], Cummings et al. [129] proposed a thermal runaway automatic detection system for lithium-ion battery cells or modules based on monitoring the gas component, which was granted a US patent in 2018. Fig. 8(c) shows the schematic diagram of the proposed alarm system [125]. Different from the apparatus proposed by Wang et al., this alarm system implemented by Cummings et al. uses a home-made SnO_2-based ceramic semiconductor gas sensor, which can detect gas concentrations in the ppb level (part per billion) and is able to detect the thermal runaway event by monitoring the vented electrolyte vapor such as DEC and DMC. This mechanism is able to detect a thermal runaway even earlier than the Figaro gas sensor, since the emission of CO and H_2 lags behind the DEC during the thermal runaway process, while the Figaro gas sensor is only able to detect the former two gases [93, 129–133]. The sequence of venting different gas components is summarized in [93] and illustrated in Table I, which can serve as a good theoretical ground to decide which specific gas sensor to choose.

The comparison result is shown in Fig. 8(d) [130] comparing the sensitivity and accuracy using the temperature sensor, the voltage sensor, and the gas sensor to monitor and detect the thermal runaway process. It can be observed that the gas sensor can detect the fault signal around 7–8 min before the actual occurrence of thermal runaway at around 10 min, which is around 2 min earlier than the voltage sensor and 7 min earlier than the temperature sensor. When a fault signal is detected, it indicates that the lithium-ion battery is undergoing the process of thermal runaway If no actions were taken in a timely manner, the thermal runaway event will further develop and intensifify, since it may only take a few minutes for a battery abuse to develop into a complete thermal runaway, and it is very difficult to suppress or mitigate the harmful consequences once the process gets started. Therefore, once the fault signal is detected, appropriate actions should be taken immediately to avoid the further development of thermal runaway.

Fig. 8(d) also indicates that the method for monitoring and detecting the thermal runaway based on gas sensors can be performed in a prognostic manner, and if an alarm can be triggered early, there would be sufficient time to turn off the battery module and protect it from developing into fires or explosions, offering significant economic savings and safety elevation for the entire battery system and human lives.

In summary, Table II shows some advantages and disadvantages of the terminal voltage and surface temperature monitoring method, the two internal state monitoring methods (including the embedded fiber sensor to measure temperature directly, and the EIS analysis method to estimate temperature indirectly), and the gas sensor monitoring method.

5. Protection methods against thermal runaway for lithium-ion batteries

In order to prevent serious consequences introduced by thermal runaway events of lithium-ion batteries, it is not only necessary to detect the thermal runaway by monitoring the status of lithium-ion batteries in real time, but it also requires taking some protective measures to

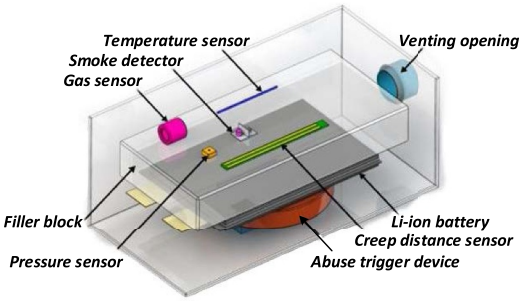

(a) Multi-sensor method [127].

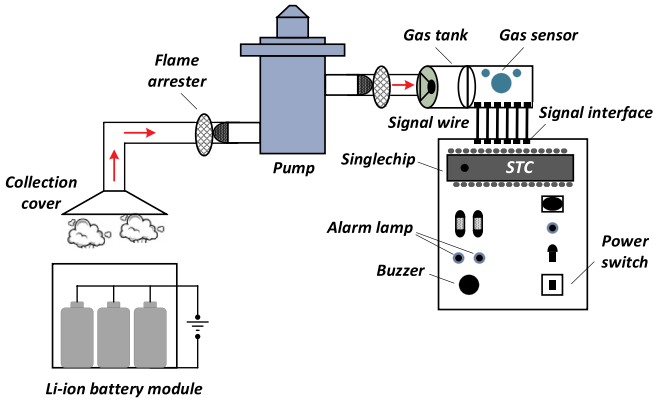

(b) Figaro gas sensor method [128].

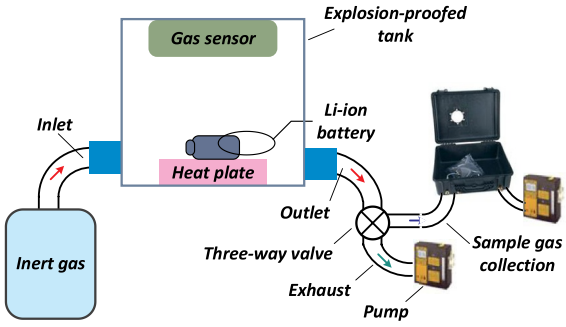

(c) Semiconductor gas sensor method [130].

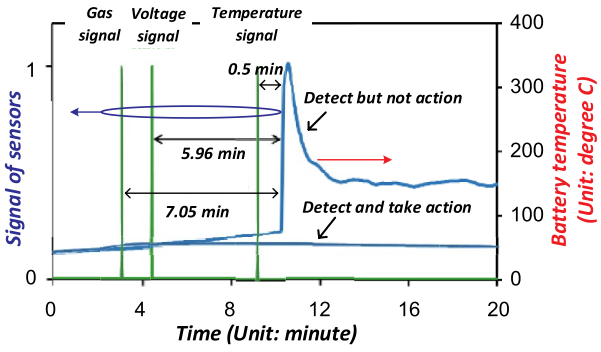

(d) Thermal runaway monitoring result based on gas sensor, voltage sensor, temperature sensor [130].

Fig. 8. Schematics of thermal runaway monitoring and detection method based on gas venting behaviors.

Table 1
A summary of gas generation during the progress of lithium-ion battery thermal runaway [88].

Time	Phenomenon
0–362 s	Lithium-ion battery working properly, no signature gas detected
362–584 s	Signature gas detected, gas concentration ranking: DMC > CO_2 > CO > EMC > CH_4
584–600 s (thermal runaway starts)	Increased gas venting rate, C_2H_4, CH_3OCH_3 and CH_3OCHO detected
600–840 s (thermal runaway peak)	Gas concentration ranking: DMC > CO_2> EMC > C_2H_4>CO > CH_3OCH_3>CH_3OCHO
840–900 s	HF detected
900–1500 s	The concentration of DMC, EMC and HF continues to rise, while other gas mixtures fall
1500–2500 s	The concentration of HF continues to rise, while other gas mixtures fall

mitigate the thermal runaway process once it occurs. Generally, it can start from two aspects to attenuate the thermal runaway process: improving the inherent safety of lithium-ion batteries at the cell level and the cooling capability at the system (module or pack) level. The cell-level safety elevation can be achieved by using safer materials and improved preparation processes for the battery itself. At the system level, protection measures include better cooling designs for effective heat dissipation and the isolation of heat propagation towards all of the neighboring cells, etc. Effective heat dissipation can rapidly cool lithium-ion batteries by forced air, liquid, and phase-change materials, thereby mitigating the thermal runaway severity. The isolation of heat propagation can prevent the thermal runaway process by blocking the heat transfer path to healthy batteries nearby, thus avoiding the domino effect or the chain reaction.

5.1. Cell-level

Based on the working principle and the thermal runaway mechanism, it is necessary and reasonable to improve the safety of lithium-ion batteries by adopting stricter preparation processes and using better materials for batteries at the cell level.

5.1.1. Reliable cathode

The excessive oxygen generated during the cathodic reaction, which can be caused by the high temperature, is one of the key issues inducing the thermal runaway process of lithium-ion batteries [134]. Therefore, enhancing the thermal stability of the cathode by doping the cathode material on the atomic level is an effective method to increase the pyrolysis temperature. However, the enhancement in the stability of cathode materials is usually accompanied by a sacrifice of the specific capacity [135,136]. Besides, another solution to improve the thermal stability of the cathode is to apply protective coatings onto the cathode surface, which can help prevent the cathode material from directly contacting the electrolyte, thereby reducing the side reaction that generates heat [137–139]. Typical protective coatings include the inorganic films (such as ZnO, Al_2O_3, AlF_3, etc.) that can conduct Li^+ after being

Table 2
Advantages and disadvantages of different methods for monitoring and detecting thermal runaway.

Method	Advantages	Disadvantages
Terminal voltage and surface temperature monitoring method	✓ Monitor the voltage and surface temperature in real-time; ✓ Capable of locating faulty battery; ✓ Predict the state of health, state of charge, etc. of the battery in real-time.	◆ Low accuracy of thermal runaway prediction; ◆ Complex topology of voltage sensors and high cost.
Embedded optical fiber sensors method	✓ Monitor the internal core temperature of the battery directly; ✓ High accuracy of thermal runaway prediction.	◆ Higher cost of embedded optical fibers; ◆ Higher requirements for battery packaging.
Electrochemical impedance spectroscopy analysis method	✓ Predict the internal core temperature of the battery without complex hardware; ✓ High accuracy of thermal runaway prediction; ✓ Predict the state of the battery on-line and seamlessly couple with the BMS.	◆ Fail to monitor large-scale batteries quickly and effectively; ◆ Complex calibration process as different lithium-ion battery systems have different parameters of impedance.
Gas sensor monitoring method	✓ High accuracy and rapid of thermal runaway detection; ✓ Simple, feasible, easy to implement and low cost; ✓ Easy to connect with the BMS interface.	◆ Fail to predict the state of the battery; ◆ Potential sensor-related faults, including gas cross-interference and gas sensor poisoning.

lithiated, the organic films (such as poly(diallyldimethylammonium chloride)), and the protective films formed by additives (such as a γ-butyrolactone, multi-component additive (composed of vinylene carbonate, 1,3-propylene sulfite, and dimethylacetamide)). In addition, the introduction of a coating having a positive temperature coefficient or a self-terminated oligomer with a hyperbranched structure is also effective at improving the safety of the cathode [140,141].

5.1.2. Reliable anode

The Lithium dendrite formed by the deposition of lithium particles on the anode surface is one of the main causes to deform the separator [142]. From the viewpoint of material properties, the most fundamental reason for the growth of lithium dendrites on the anode surface is the uneven anode current distribution caused by the instability and inhomogeneity of the SEI. The formation of lithium dendrites can be alleviated by improving the anode material [143,144], such as the silicon-based material and the graphite carbon material, or cover the anode surface with protective coatings. However, when lithium-ion batteries are subjected to impacts from an abuse, such as overcharging or overdischarging, the distribution of lithium ions close to the anode is uneven due to the uneven distribution of the anode current, and lithium ions are reduced to lithium particles, which are deposited on the anode surface to form lithium dendrites. In order to inhibit the growth of lithium dendrites caused by the uneven formation of SEI, a mainstream solution is to add electrolyte additives to stabilize the interface between the anode and the electrolyte.

Specifically, certain additives attached to the anode surface can serve as one type of reactants in the formation of SEI (or modify its physical and chemical properties) through decomposition or polymerization. Therefore, the reactivity of the anode can be changed, and the current distribution can be adjusted in the process of lithium deposition. Following this path, these additives can also make lithium ions uniformly deposited on the anode surface, thus avoiding the formation of lithium dendrites. Even if these additives in the electrolyte is only at the ppm level, it can improve the morphology of the lithium deposition. Typical electrolyte additives for stabilizing the interface between the anode and the electrolyte include the inorganic compound (such as CO_2, LiI, etc.), the organic compound containing unsaturated carbon bonds (such as vinyl carbonate, maleimide, etc.), the unstable cyclic molecules (such as butyrolactone, ethylene sulfite, etc.), and the fluoride carbonate [19].

5.1.3. Non-flammable electrolyte

The electrolyte is in charge of migrating lithium ions between the cathode and the anode in lithium-ion batteries. However, the traditional carbonate electrolyte is flammable. In order to reduce the risk of thermal runaway and enhance the thermal robustness of lithium-ion batteries, another effective strategy is to improve the thermal stability of lithium salts, as well as the fire retardancy and heat resistance of the electrolyte.

To improve the thermal stability of lithium salts, researchers substituted fluorine atoms in conventional $LiPF_6$ by alkyl or alkoxy groups to obtain certain lithium salt derivatives, such as the polyfluoroalkylamide lithium salt and the polyfluoro-alkoxyimide lithium salt, the new material has a similar conductivity, a higher flash point, a stronger thermal stability, more stable chemical properties, and it is harder to hydrolyze when compared to the conventional $LiPF_6$ [145–147].

Furthermore, in order to tackle problems associates to the carbonate solvent electrolyte, a significant amount of progress has been made to improve the heat resistance and non-flammability of the electrolyte by adding flame retardant electrolyte additives [148], choosing the phosphate organic solvent [149], and adjusting the ratio of the lithium salt to the electrolyte solvent [150]. Pham et al. [148] added the fluorinated diethyl carbonate additive to the traditional carbonate electrolyte (with PC as the solvent and $LiPF_6$ as the lithium salt), which can suppress the flammability of the electrolyte by combining fluoride ions with hydrogen ions during the electrolyte combustion. In addition, for the phosphate electrolyte, Pires et al. [151] used the tris(2,2,2-trifluoroethyl) phosphite as an additive in the EC/DMC 1 M $LiPF_6$ electrolyte. It is found that the partial fluorination of the alkyl phosphate can improve the cycle performance of batteries, the formation of SEI, and the deactivation of PF_5, thereby enhancing the non-flammability of the cathode/electrolyte and improving the safety of lithium-ion batteries.

Moreover, Jin et al. [152] used a synthesized bi-functional additive, specifically, the bis(2-methoxyethoxy) methylallyl phosphonate, as the flame retardant and film-forming agent in the EC/DMC 1 M $LiPF_6$ electrolyte, then the flame retardancy of the additive was characterized by measuring the self-extinguishing time of the electrolyte. The result shows that the bis(2-methoxyethoxy) methylallyl phosphonate exhibits a good electrochemical compatibility with the graphite anode, as well as enhancements to the thermal stability of the electrolyte. Furthermore, Zeng et al. [150] used the phosphate organic solvent and the high-concentration LiFSI (bis(fluorosulfony)imide lithium) salt as the flame-retardant additive to the electrolyte. Solvent molecules and lithium ions can form a solvation shell during the combustion of the electrolyte, simultaneously maintaining the non-flammability of the electrolyte and improving the coulombic efficiency and the cycle stability of lithium-ion batteries.

5.1.4. Thermally stable separator

The separator is a key component for the safety of lithium-ion batteries, since it is able to prevent the direct electrical contact between the

high-energy cathode and anode materials, while allowing lithium ions to migrate. Although PP and PE are the most commonly used materials, they come with poor thermal stabilities as their melting points are only around 165 °C and 135 °C, respectively. For a commercial PP/PE/PP three-layer separator, PE is the intermediate protection layer. When the internal temperature of a lithium-ion battery rises above the critical temperature (around 130 °C), the porous PE layer will partially melt, blocking the pores of the separator and preventing the migration of lithium ions in the electrolyte, while the PP layer provides the mechanical support necessary to avoid an internal short-circuit fault.

To summarize, methods improving the thermal stability of the separator and thus the safety of lithium-ion batteries are:

(1) Coating or enlarging the inorganic ceramic layer (with SiO_2, Al_2O_3, etc.) on the surface of the separator to improve its mechanical strength and insulation propertie;
(2) Filling the micro-porous separator with gel, which can effectively prevent the short-circuiting between the cathode and anode caused by the shrinkage of the separator at a high temperature;
(3) Compounding nano-oxides and nitrides on the nanocellulose to form a non-woven nanofiber separator that improves the thermal stability of the separator;
(4) Compounding a variety of polymers to form a microporous polymer separator with a self-sealing mechanism at high temperatures, the micropore can be blocked by the low-melting-point polymer when the separator is overheated;
(5) Adopting modified polysiloxane solvents and inorganic fillers as separator additives, preventing the short-circuiting between the cathode and anode at a high temperature.

5.1.5. Preparation process

In addition to the battery material, there are many factors affecting the safety and robustness of lithium-ion batteries during their manufacturing process, such as the micro-metal impurity, the uniformity of the slurry coating of the electrode plate, the residual moisture concentration, and the electrolyte dosage, etc. Among them, moisture has a vital impact on the safety of lithium-ion batteries, so it must be strictly controlled during the entire manufacturing process.

Besides accelerating the decomposition of lithium salts in the electrolyte that produces gas, the excessive residual moisture in lithium-ion batteries also has certain corrosive and destructive effects on the cathode, the anode, and the collector. When lithium-ion batteries are charging or discharging, the moisture can react with the lithium to form the lithium oxide, which can reduce the battery capacity and increase the risk of a battery overcharge.

In addition, if the slurry coating of the electrode paste is not uniform, the polarization of the anode would vary from place to place throughout the lithium-ion battery charging process, which can further induce the deposition of lithium on the anode surface. Therefore, the key to prevent the formation of lithium dendrites is to appropriately control the proportion of the cathode and anode materials and enhance the uniformity of the slurry coating.

5.2. System-level

Many lithium-ion battery applications, such as the energy storage station and the power unit of electric vehicles, are modules composed of a large number of lithium-ion battery cells connected in series and in parallel, all stacked inside a specific container. If one lithium-ion battery cell in the container happens to have a thermal runaway failure, all of the neighboring cells will be in risk due to the small and enclosed container space that limits the heat dissipation and intensifies the heat transfer among different battery cells. If no protection measures were taken at an early stage, all of the lithium-ion battery cells in the container will ultimately experience the thermal runaway failure due the domino effect. Therefore, in order to mitigate concerns and consequences related to thermal runaway, an effective thermal management system is typically designed and integrated into a lithium-ion battery system, which includes methodologies for effective heat dissipation and isolation of thermal propagation, etc.

5.2.1. Heat dissipation technology

Through active interventions, effective heat dissipation methodologies are able to regulate the temperature of battery packs within the safety range, thus suppressing the occurrence and propagation of a thermal runaway event. In addition, it is also able to reduce the temperature difference among different battery cells in a battery pack, alleviating the concern for certain extremely hot local spots and enhancing the overall robustness of the lithium-ion battery system.

From the safety point of view, the development of heat dissipation technologies for lithium-ion battery systems mainly focuses on the enhancement of heat dissipation capabilities, the improvement on the uniformity of the individual cell temperature, and the improvement on the heat dissipation reliability. Typical heat dissipation technologies used in lithium-ion battery systems mainly include the air cooling (including the natural and forced-air cooling) [153], the phase change/heat pipe cooling (using the rapid heat transfer properties of phase change materials) [154,155], and the liquid cooling (using a pump to circulate a coolant in the pipe for heat dissipation) [156]. Readers are referred to several recent review papers [157–161] for a more detailed analysis and comparison on the existing heat dissipation methodologies.

5.2.2. Heat isolation technology

The heat isolation technology can prevent the spread of heat and the ejected high-temperature substances during the thermal runaway process, thereby mitigating the propagation of thermal runaway events. The propagation of thermal runaway can be mainly attributed to: 1) the flame and high-temperature substances ejected by the faulty cell during an explosion or valve spray, which can directly heat all of the neighboring cells, and 2) the heat transmission and the mechanical impact generated by the faulty cell. In order to block the propagation of thermal runaway, various heat isolation methods have been applied to the lithium-ion battery system, which can be mainly categorized into the blocking structure for heat transfer and the venting valve channel.

For various applications involving the blocking structure for heat transfer, Tesla Inc [162–165]. placed a multi-layer thermal barrier to reduce the heat transfer and the mechanical impact among different battery cells and modules in an electric vehicle battery pack. Specifically, a multi-layer thermal barrier, which is made of a composite material consisting of thermal insulation materials and elastic materials, is inserted between each pair of battery cells and arrays to prevent the propagation of thermal runaway events. In addition, Berdichevsky et al. [166] added a heat-conducting plate on the outer wall of the lithium-ion battery array, aiming at enhancing the heat transfer capability between the battery array and the cooling medium. In addition, they also placed an adiabatic flame-retardant plate and an anti-radiation metal plate between each pair of battery arrays to reduce the thermal conduction and radiation, thereby blocking the thermal runaway propagation. Moreover, Rawlinson et al. [167] placed several hollow beams loaded with liquid materials (with a high melting point and a low thermal conductivity) in a lithium-ion battery system, which can divide a battery pack into several groups and subsequently inhibit the thermal runaway propagation within these groups. Additionally, the mechanical impact produced during thermal runaway can be uniformly allocated to these hollow beams. Therefore, the influence of the thermal and mechanical impact of the faulty battery on other healthy batteries can be effectively mitigated.

Besides, for a lithium-ion battery cell undergoing the thermal runaway process, the ejected high-temperature substance and flame will spray onto other healthy lithium-ion battery cells, which is the main cause for the propagation of thermal runaway. However, a good design

of the venting valve channel can physically isolate this influence. Consequently, Chow et al. [168] designed a unique venting valve channel for each battery cell in a lithium-ion battery system, so a faulty battery cell can emit the high-temperature substance from their unique venting valve channels without affecting other healthy batteries. To avoid any malfunction of the venting valve channel itself, Hore et al. [169] proposed a methodology to detect whether the safety valve of each battery cell was flushed away by high-temperature substances. If this is the case, external CO_2 will be injected into the lithium-ion battery system to expel, dilute, and cool these substances and revitalize the venting valve channel.

6. Conclusions and outlook

As lithium-ion batteries find increasing popularity, safety concerns characterized by the thermal runaway event have become a life-threatening issue in many applications and have become a major challenge for both industry and academia. Many feasible solutions for detecting a thermal runaway process are based on monitoring certain characteristic fault signals, including the terminal voltage, the surface/inner temperature and the vented gas.

For the terminal voltage and surface temperature monitoring method, improving the precision of voltage sensors and temperature sensors in the BMS can enhance the thermal runaway detection accuracy. In addition, both the hardware and software solutions can be designed to optimize the sensor array topology with a minimum number of sensors and an intelligent measurement/control strategy.

Similarly, for the internal state prediction method, it is necessary to improve the detection resolution and the high temperature resistance of sensors embedded in the battery, as well as the sealing of the lithium-ion battery packaging, to ensure the electrolyte will not leak. Finally, the internal state prediction method can be coupled with BMS to establish a more accurate risk assessment model for thermal runaway of lithium-ion batteries.

Monitoring the thermal runaway process with gas sensors has been shown as a more effective method than with voltage sensors or temperature sensors. However, depending on the working principle of a specific sensor, such as the electrochemical or semiconductor gas sensor, etc., there are still many sensor-related problems including the low detection accuracy, the complex gas cross-interference, and the gas sensor poisoning. Therefore, the development of new types of portable gas sensors, such as the MEMS micro-optical gas sensor, the photo-acoustic spectrometer, and the infrared spectrometer, can be beneficial in generating an accurate early-warning signal for applications involving lithium-ion batteries that can run into a thermal runaway problem.

The purpose of monitoring and detecting the status of lithium-ion batteries is to warn the potential risk of a thermal runaway event in lithium-ion battery systems. Apart from these monitoring schemes, more attempts can be also made to improve the inherent safety of the lithium-ion battery itself, such as using safer materials and improving the quality of the preparation process. In addition, many protection measures can be also designed at the battery system level by adopting more effective heat dissipation and heat isolation methodologies to restrain the occurrence and the spread of thermal runaway events.

From the material point of view, to further improve battery safeties, the cathode material with a higher heat resistance and the anode material capable of suppressing the accumulation of lithium dendrites are vital goals for the next-generation electrode materials. Most of the recent research work on the non-flammable electrolyte are focused on the flame-retardant additive, which would help decrease the conductivity of the electrolyte and inhibit the formation of the SEI layer on the anode surface, but it comes with a cost of decreasing the coulombic efficiency of lithium-ion batteries. Therefore, the main goal for developing the future non-flammable electrolyte would be: 1) ensuring the high flame retardancy of the electrolyte; 2) improving the stability of the electrolyte and anode interface; and 3) enhancing the battery coulombic efficiency. Furthermore, in terms of improving the heat dissipation and thermal isolation technologies, it is necessary to improve the performance and reliability of the cooling design with an effective mechanical structure. Ultimately, with the proper implementation of the aforementioned measures, only minor temperature deviations will be present among all of the battery cells in a lithium-ion battery system.

Acknowledgments

This research is supported by the National Natural Science Foundation of China (51877203), and the Science and Technology Foundation of State Grid Corporation of China (521205190014).

References

[1] Y. Nishi, Lithium ion secondary batteries; past 10 years and the future, J. Power Sources 100 (2001) 101–106.
[2] P.J. Bugrynieca, J.N. Davidsonb, D.J. Cumming, et al., Pursuing safer batteries: thermal abuse of $LiFePO_4$ cells, J. Power Sources 414 (2019) 557–568.
[3] G.E. Blomgren, The development and future of lithium ion batteries, J. Electrochem. Soc. 164 (1) (2017) A5019–A5025.
[4] J.-M. Tarascon, M. Armand, Issues and challenges facing rechargeable lithium batteries, Nature 414 (6861) (2001) 359–367.
[5] J.B. Goodenough, Y. Kim, Challenges for rechargeable Li batteries, Chem. Mater. 22 (2010) 587–603.
[6] D. Lyu, B. Ren, S.F. Li, Failure modes and mechanisms for rechargeable Lithium-based batteries: a state-of-the-art review, Acta Mech. 230 (3) (2019) 701–727.
[7] A. Yoshino, Development of the lithium-ion battery and recent technological trends, in: G. Pistoia (Ed.), Lithium-Ion Batteries, Elsevier, Amsterdam, 2014, pp. 1–20.
[8] Chinese reports, The market value of lithiumion batteries [Online]. Available: http://market.chinabaogao.com/nengyuan/0212320L42018.html, 2018. (Accessed April 2019).
[9] X.N. Feng, M.G. Ouyang, X. Liu, et al., Thermal runaway mechanism of lithium ion battery for electric vehicles: a review, Energy Storage Mater. 10 (2018) 246–267.
[10] D. Deng, lithium-ion batteries: basics, progress, and challenges, Energy Sci. Eng. 3 (5) (2015) 385–418.
[11] T. Yamanaka, Y. Takagishi, Y. Tzuka, et al., Modeling lithium ion battery nail penetration tests and quantitative evaluation of the degree of combustion risk, J. Power Sources 416 (2019) 132–140.
[12] R. Spotnitz, J. Franklin, Abuse behavior of high-power, lithium-ion cells, J. Power Sources 113 (1) (2003) 81–100.
[13] D.X. Ouyang, M.Y. Chen, J.H. Liu, et al., Investigation of a commercial lithium-ion battery under overcharge/over-discharge failure conditions, RSC Adv. 8 (58) (2018) 33414–33424.
[14] M. Henriksen, K. Vaagsaether, J. Lundberg, et al., Explosion characteristics for lithium-ion battery electrolytes at elevated temperatures, J. Hazard Mater. 371 (2019) 1–7.
[15] J. Sun, J.G. Li, T. Zhou, et al., Toxicity, a serious concern of thermal runaway from commercial lithium-ion battery, Nano Energy 27 (2016) 313–319.
[16] ISO 12405-3:2014, Electrically propelled road vehicles–test specification for lithium-ion traction battery packs and systems–part 3: safety performance requirements [Online]. Available: https://www.iso.org/standard/59224.html.
[17] IEC 62133.2-2017, Secondary Cells and Batteries Containing Alkaline or Other Non - Acid Electrolytes–Safety Requirements for Portable Sealed Secondary Cells, and for Batteries Made from Them, for Use in Portable Applications - Part 2: Lithium Systems [Online]. Available: https://webstore.iec.ch/publication/32662.
[18] Q.S. Wang, P. Ping, X.J. Zhao, et al., Thermal runaway caused fire and explosion of lithium ion battery, J. Power Sources 208 (2012) 210–224.
[19] K. Liu, Y.Y. Liu, D.C. Lin, et al., Materials for lithium-ion battery safety, Sci. Adv. 4 (2018) 1–11.
[20] R. Guo, L.G. Lu, M.G. Ouyang, X.N. Feng, Mechanism of the entire overdischarge process and overdischarge-induced internal short circuit in lithium-ion batteries, Sci. Rep. 6 (30248) (2016) 1–9.
[21] G. Gachot, P. Ribière, D. Mathiron, et al., Gas chromatography/mass spectrometry as a suitable tool for the li-ion battery electrolyte degradation mechanisms study, Anal. Chem. 83 (2) (2011) 478–485.
[22] M. Lammer, A. Konigseder, V. Hacker, Holistic methodology for characterisation of the thermally induced failure of commercially available 18650 lithium ion cells, R. Soc. Chem. Adv. 7 (2017) 24425–24429.
[23] J.N. Zhang, L. Zhang, F.C. Sun, et al., An overview on thermal safety issues of lithium-ion batteries for electric vehicle application, IEEE Access 6 (2018) 23848–23863.
[24] J.W. Wen, Y. Yu, C.H. Chen, A review on lithium-ion batteries safety issues: existing problems and possible solutions, Mater. Express 2 (3) (2012) 197–212.
[25] T.M. Bandhauer, S. Garimella, T.F. Fuller, A critical review of thermal issues in lithium-ion batteries, J. Electrochem. Soc. 158 (3) (2011) R1–R25.

[26] S. Abada, G. Marlair, A. Lecocq, et al., Safety focused modeling of lithium-ion batteries: a review, J. Power Sources 306 (2016) 178–192.
[27] X. Michaud, K. Shi, I. Zhitomirsky, Electrophoretic deposition of $LiFePO_4$ for Li-ion batteries, Mater. Lett. 241 (2019) 10–13.
[28] D. Choi, J. Kang, B. Han, Unexpectedly high energy density of ali-ion battery by oxygen redox in $LiNiO_2$ cathode: first-principles study, Electrochim. Acta 294 (2019) 166–172.
[29] C. Jiang, Z. Tang, S. Deng, et al., High performance carbon-coated mesoporous $LiMn_2O_4$ cathode materials synthesized from a novel hydrated layered-spinel lithium manganate composite, RSC Adv. 7 (7) (2017) 3746–3751.
[30] Z. Jian, W. Wang, M. Wang, et al., Al_2O_3 coated $LiCoO_2$ as cathode for high-capacity and long cycling Li-ion batteries, Chin. Chem. Lett. 29 (12) (2018) 1768–1772.
[31] J. Liu, Y. Chen, J. Xu, et al., Effectively enhanced structural stability and electrochemical properties of $LiNi_{0.5}Mn_{1.5}O_4$ cathode materials via poly-(3, 4-ethylenedioxythiophene)-in situ coated for high voltage Li-ion batteries, RSC Adv. 9 (6) (2019) 3081–3091.
[32] M. Zhang, M. Chen, Y. Shao, et al., Enhanced performance of $LiNi_{0.03}Mo_{0.01}Mn_{1.96}O_4$ cathode materials coated with biomass-derived carbon layer, Ionics 25 (3) (2019) 917–925.
[33] T. Weigel, F. Schipper, E.M. Erickson, et al., Structural and electrochemical aspects of $LiNi_{0.8}Co_{0.1}Mn_{0.1}O_2$ cathode materials doped by various cations, ACS Energy Lett. 4 (2) (2019) 508–516.
[34] D.J. Li, H. Li, L.D. Dmitri, et al., Degradation mechanisms of C_6/$LiNi_{0.5}Mn_{0.3}Co_{0.2}O_2$ lithium-ion batteries unraveled by non-destructive and post-mortem methods, J. Power Sources 416 (2019) 163–174.
[35] Z.W. Wu, C.H. Cao, X.D. Yan, et al., Effects of charge cut-off voltage on the performances of monocrystalline $LiNi_{0.5}Co_{0.2}Mn_{0.3}O_2$/graphite lithium-ion cells, Electrochim. Acta 302 (2019) 153–160.
[36] K. Sahni, M. Ashuri, Q.R. He, et al., H3PO4 treatment to enhance the electrochemical properties of $Li(Ni_{1/3}Mn_{1/3}Co_{1/3})O_2$ and $Li(Ni_{0.5}Mn_{0.3}Co_{0.2})O_2$ cathodes, Electrochim. Acta 301 (2019) 8–22.
[37] H.-J. Noh, S. Youn, S.Y. Chong, et al., Comparison of the structural and electrochemical properties of layered $Li[Ni_xCo_yMn_z]O_2$ (x = 1/3, 0.5, 0.6, 0.7, 0.8 and 0.85) cathode material for lithium-ion batteries, J. Power Sources 233 (2013) 121–130.
[38] Y. Li, H. Huang, J.G. Yu, et al., Improved high rate capability of Li $[Li_{0.2}Mn_{0.534}Co_{0.133}Ni_{0.133}]O_2$ cathode material by surface modification with Co3O4, J. Alloy. Comp. 783 (2019) 349–356.
[39] Z. Zhang, Y. Huang, J. Yan, et al., A facile synthesis of 3D flower-like $NiCo_2O_4$@ MnO_2 composites as an anode material for lithium-ion batteries, Appl. Surf. Sci. 473 (2019) 266–274.
[40] Q. Li, G.Z. Zhu, Y.H. Zhao, et al., $Ni_xMn_yCo_zO$ nanowire/CNT composite microspheres with 3D interconnected conductive network structure via spray-drying method: a high-capacity and long-cycle-life anode material for lithium-ion batteries, Small (2019), e1805173.
[41] Y. Ding, D.B. Mu, B.R. Wu, et al., Recent progresses on nickel-rich layered oxide positive electrode materials used in lithium-ion batteries for electric vehicles, Appl. Energy 195 (2017) 586–599.
[42] A. Manthiram, B.H. Song, W.D. Li, A perspective on nickel-rich layered oxide cathodes for lithium-ion batteries, Energy Storage Mater. 6 (2017) 125–139.
[43] Q. Wu, K. Xue, X.H. Zhang, et al., Enhanced cyclic stability at elevated temperature of spinel $LiNi_{0.5}Mn_{1.5}O_4$ by $Li_4Ti_5O_{12}$ coating as cathode material for high voltage lithium ion batteries, Ceram. Int. 54 (4) (2019) 5072–5079.
[44] S. Deng, Y. Zhang, D. Xie, et al., Oxygen vacancy modulated $Ti_2Nb_{10}O_{29-x}$ embedded onto porous bacterial cellulose carbon for highly efficient lithium ion storage, Nano Energy 58 (2019) 355–364.
[45] S. Shen, W. Guo, D. Xie, et al., A synergistic vertical graphene skeleton and S-C shell to construct high-performance $TiNb_2O_7$-based core/shell arrays, J. Mater. Chem. 6 (2018) 20195–20204.
[46] Z. Yao, X. Xia, D. Xie, et al., Enhancing ultra-fast lithium ion storage of $Li_4Ti_5O_{12}$ by tailored TiC/C core/shell skeleton plus nitrogen doping, Adv. Funct. Mater. 28 (31) (2018) 1802756.
[47] S. Deng, D. Chao, Y. Zhong, et al., Vertical graphene/$Ti_2Nb_{10}O_{29}$/hydrogen molybdenum bronze composite arrays for enhanced lithium ion storage, Energy Storage Mater. 12 (2018) 137–144.
[48] X. Xia, S. Deng, S. Feng, et al., Hierarchical porous $Ti_2Nb_{10}O_{29}$ nanospheres as superior anode materials for lithium ion storage, J. Mater. Chem. 5 (2017) 21134–21139.
[49] A. Samad, H.J. Kim, Y.-H. Shin, Structure stability and high Li storage capacity of the unzipped graphene oxide monolayer, Appl. Surf. Sci. 475 (2019) 151–157.
[50] M.K. Aslam, S.S. A Shah, T. Najam, et al., Decoration of cobalt/iron oxide nanoparticles on N-doped carbon nanosheets: electrochemical performances for lithium-ion batteries, J. Appl. Electrochem. 49 (4) (2019) 433–442.
[51] S.Y. Zhou, Z.W. Zheng, T. Mei, et al., Structural design and material preparation of carbon-based electrodes for high-performance lithium storage systems, Carbon 144 (2019) 127–146.
[52] Z.Y. Xia, M. Christian, C. Arbizzani, et al., A robust, modular approach to produce graphene-MOx multilayer foams as electrodes for lithium-ion batteries, Nanoscale 11 (12) (2019) 526–5273.
[53] D.X. Yang, H.Y. Ren, D.P. Zhang, et al., Bi-functional nitrogen-doped carbon protective layer on three-dimensional RGO/SnO_2 composites with enhanced electron transport and structural stability for high-performance lithium-ion batteries, J. Colloid Interface Sci. 542 (2019) 81–90.
[54] T.T. Ma, L. Sun, Q. Niu, et al., N-doped carbon-coated Tin sulfide/graphene nanocomposite for enhanced lithium storage, Electrochim. Acta 300 (2019) 131–137.
[55] T. Izawa, A.F. Arif, S. Taniguchi, et al., Improving the performance of lithium-ion battery carbon anodes by in-situ immobilization of SiOx nanoparticles, Mater. Res. Bull. 112 (2019) 16–21.
[56] N. Umirov, D.-H. Seo, T. Kim, et al., Microstructure and electrochemical properties of rapidly solidified Si-Ni alloys as anode for lithium-ion batteries, J. Ind. Eng. Chem. 71 (2019) 351–360.
[57] N.P. Wagner, A. Tron, J.R. Tolchard, et al., Silicon anodes for lithium-ion batteries produced from recovered kerf powders, J. Power Sources 414 (2019) 377–382.
[58] H. Li, B. Zhang, Q.J. Zhou, et al., Dual-carbon confined SnO2 as ultralong-life anode for lithium-ion batteries, Ceram. Int. 45 (6) (2019) 7830–7838.
[59] L. Sun, H.C. Si, Y.X. Zhang, et al., Sn-SnO2 hybrid nanoclusters embedded in carbon nanotubes with enhanced electrochemical performance for advanced lithium ion batteries, J. Power Sources 415 (2019) 126–135.
[60] W.T. Zhang, X. Yu, Z.Q. Guo, et al., Magnetron sputtering deposition of MSb (M=Fe, Ni, Co) thin films as negative electrodes for lithium-ion and Na-ion batteries, Mater. Res. Express 6 (5) (2019), 056410.
[61] J.-S. Park, J.S. Cho, Y.C. Kang, Nickel vanadate microspheres with numerous nanocavities synthesized by spray drying process as an anode material for lithium-ion batteries, J. Alloy. Comp. 780 (2019) 948–958.
[62] A.T. Tesfaye, F. Dumur, D. Gigmes, et al., Superior electrochemical performance of thin-film thermoplastic elastomer-coated SnSb as an anode for lithium-ion batteries, Sci. Rep. 9 (2019) 4301.
[63] F. Ahmed, M.M. Rahman, S.C. Sutradhar, et al., Synthesis and electrochemical performance of an imidazolium based Li salt as electrolyte with Li fluorinated sulfonylimides as additives for Li-Ion batteries, Electrochim. Acta 302 (2019) 161–168.
[64] E. Kowsari, P. Salimi, Electrochemical study of Li-ion 18650 cylindrical rechargeable cell at elevated temperature using geminal dicationic ionic liquid as electrolyte additive, J. Electron. Mater. 48 (4) (2019) 2254–2262.
[65] D.S. Hall, J. Li, K. Lin, et al., A Tale of Two Additives: effects of glutaric and citraconic anhydrides on lithium-ion cell performance, J. Electrochem. Soc. 166 (4) (2019) A793–A801.
[66] G.J. Xu, S.Q. Huang, Z.L. Cui, et al., Functional additives assisted ester-carbonate electrolyte enables wide temperature operation of a high-voltage (5 V-Class) lithium-ion battery, J. Power Sources 416 (2019) 29–36.
[67] Q.Q. Zhang, K. Liu, F. Ding, et al., Enhancing the high voltage interface compatibility of $LiNi_{0.5}Co_{0.2}Mn_{0.3}O_2$ in the succinonitrile-based electrolyte, Electrochim. Acta 298 (2019) 818–826.
[68] P. Zhao, J.P. Yang, Y.M. Shang, et al., Surface modification of polyolefin separators for lithium ion batteries to reduce thermal shrinkage without thickness increase, J. Energy Chem. 24 (2) (2015) 138–144.
[69] H. Jeon, Y. Roh, D. Jin, et al., Crosslinkable polyhedral silsesquioxane-based ceramic-coated separators for lithium-ion batteries, J. Ind. Eng. Chem. 71 (2019) 277–283.
[70] A.K. Padh, K.S. Nanjundaswamy, J.B. Goodenough, Phospho-olivines as positive-electrode materials for rechargeable lithium batteries, J. Electrochem. Soc. 144 (1997) 1188–1194.
[71] B. Mao, H. Chen, Z. Cui, et al., Failure mechanism of the lithium ion battery during nail penetration, Int. J. Heat Mass Transf. 122 (2018) 1103–1115.
[72] M. Chen, F. Bai, S. Lin, et al., Performance and safety protection of internal short circuit in lithium-ion battery based on a multilayer electro-thermal coupling model, Appl. Therm. Eng. 146 (2019) 775–784.
[73] D.P. Finegan, E. Darcy, M. Keyser, et al., Characterising thermal runaway within lithium-ion cells by inducing and monitoring internal short circuits, Energy Environ. Sci. 10 (6) (2017) 1377–1388.
[74] J.M. Sherfey, A. Brenner, Electrochemical calorimetry, J. Electrochem. Soc. 105 (11) (1958) 665–672.
[75] S. Gross, Heat generation in sealed batteries, Energy Convers. 9 (2) (1969) 55–62.
[76] H.F. Gibbard, Thermal properties of battery systems, J. Electrochem. Soc. 125 (3) (1978) 353–358.
[77] D. Bernardi, E. Pawlikowski, J. Newman, A general energy balance for battery systems, J. Electrochem. Soc. 132 (1) (1985) 5–12.
[78] T.D. Hatchard, D.D. MacNeil, A. Basu, et al., Thermal model of cylindrical and prismatic lithium-ion cells, J. Electrochem. Soc. 148 (7) (2001) A755–A761.
[79] P.F. Huang, H.D. Chen, A. Verma, et al., Non-dimensional analysis of the criticality of lithium-ion battery thermal runaway behavior, J. Hazard Mater. 369 (2019) 268–278.
[80] X.N. Feng, M. Feng, X.M. He, et al., Thermal runaway features of large format prismatic lithium ion battery using extended volume accelerating rate calorimetry, J. Power Sources 255 (2014) 294–301.
[81] D. Doughty, E.P. Roth, A general discussion of li ion battery safety, Electrochem. Soc. Interface 21 (2012) 37–44.
[82] K. Xu, G.R.V. Zhuang, J.L. Allen, et al., Syntheses and characterization of lithium alkyl mono- and dicarbonates as components of surface films in li-ion batteries, J. Phys. Chem. B 110 (2006) 7708–7719.
[83] G.R.V. Zhuang, H. Yang, P.N. Ross, et al., Lithium methyl carbonate as a reaction product of metallic lithium and dimethyl carbonate, Electrochem. Solid State Lett. 9 (2) (2006) A64–A68.
[84] M.N. Richard, J.R. Dahn, Accelerating rate calorimetry study on the thermal stability of lithium intercalated graphite in electrolyte. I. experimental, J. Electrochem. Soc. 146 (6) (1999) 2068–2077.

[85] K. Zaghib, J. Dubé, A. Dallaire, et al., Enhanced thermal safety and high power performance of carbon-coated LiFePO4 olivine cathode for lithium-ion batteries, J. Power Sources 219 (2012) 36–44.

[86] H. Yoshida, T. Fukunaga, T. Hazama, et al., Degradation mechanism of alkyl carbonate solvents used in lithium-ion cells during initial charging, J. Power Sources 68 (1997) 311–315.

[87] E.S. Takeuchi, H. Gan, M. Palazzo, et al., Anode passivation and electrolyte solvent disproportionation: mechanism of ester exchange reaction in lithium-ion batteries, J. Electrochem. Soc. 144 (6) (1997) 1944–1948.

[88] H. Arai, M. Tsuda, K. Saito, et al., Thermal reactions between de- lithiated lithium nickelate and electrolyte solutions, J. Electrochem. Soc. 149 (2002) A401–A406.

[89] S. Solchenbach, M. Metzger, M. Egawa, et al., Quantification of PF5 and POF3 from side reactions of LiPF6 in Li-ion batteries, J. Electrochem. Soc. 165 (13) (2018) A3022–A3028.

[90] A.D. Pasquier, F. Disma, T. Bowmer, Differential scanning calorimetry study of the reactivity of carbon anodes in plastic li-ion batteries, J. Electrochem. Soc. 145 (2) (1998) 472–477.

[91] R. Hausbrand, G. Cherkashinin, H. Ehrenberg, et al., Fundamental degradation mechanisms of layered oxide lithium-ion battery cathode materials: methodology, insights and novel approaches, Mater. Sci. Eng., B 192 (2015) 3–25.

[92] Y. Fernandes, A. Brya, S. de Persis, Thermal degradation analyses of carbonate solvents used in lithium-ion batteries, J. Power Sources 414 (2019) 250–261.

[93] Y. Fernandes, A. Bry, S. de Persis, Identification and quantification of gases emitted during abuse tests by overcharge of a commercial lithium-ion battery, J. Power Sources 389 (2018) 106–119.

[94] S. Koch, A. Fill, K.P. Birke, Comprehensive gas analysis on large scale automotive lithium-ion cells in thremal runaway, J. Power Sources 398 (2018) 106–112.

[95] W.Q. Walker, J.J. Darst, D.P. Finegan, et al., Decoupling of heat generated from ejected and non-ejected contents of 18650-format lithium-ion cells using statistical methods, J. Power Sources 415 (2019) 207–218.

[96] K. Smith, G.-H. Kim, E. Darcy, al er, Thermal/electrical modeling for abuse-tolerant design of lithium ion modules, Int. J. Energy Res. 34 (2) (2010) 204–215.

[97] D.X. Ouyang, J.H. Liu, W.Y. Chen, et al., An experimental study on the thermal failure propagation in lithium-ion battery pack, J. Electrochem. Soc. 165 (10) (2018) A2184–A2193.

[98] J. Lamb, C.J. Orendorff, L.A.M. Steele, et al., Failure propagation in multi-cell lithium ion batteries, J. Power Sources 283 (2015) 517–523.

[99] X.N. Feng, L.G. Lu, M.G. Ouyang, et al., A 3D thermal runaway propagation model for a large format lithium ion battery module, Energy 115 (2016) 194–208.

[100] K.L. Liu, K. Li, Q. Peng, et al., A brief review on key technologies in the battery management system of electric vehicles, Front. Mech. Eng. 14 (1) (2019) 47–64.

[101] G.S. Misyris, D.I. Doukas, T.A. Papadopoulos, et al., State-of-charge estimation for lithium-ion batteries: a more accurate hybrid approach, IEEE Trans. Energy Convers. 34 (1) (2019) 109–119.

[102] R. Xiong, L.L. Li, J.P. Tian, Towards a smarter battery management system: a critical review on battery state of health monitoring methods, J. Power Sources 405 (2018) 18–29.

[103] B. Xia, C. Mi, A fault-tolerant voltage measurement method for series connected battery packs, J. Power Sources 308 (2016) 83–96.

[104] B. Xia, T. Nguyen, J. Yang, et al., The improved interleaved voltage measurement method for series connected battery packs, J. Power Sources 334 (2016) 12–22.

[105] B. Xia, Y. Shang, T. Nguyen, et al., A correlation based fault detection method for short circuits in battery packs, J. Power Sources 337 (2017) 1–10.

[106] EVTV monitor/controller for tesla model s battery modules [Online]. Available: http://media3.ev-tv.me/TeslaModuleController.pdf. (Accessed April 2019).

[107] M. Nascimento, M.S. Ferreira, J.L. Pinto, Real time thermal monitoring of lithium batteries with fiber sensors and thermocouples: a comparative study, Measurement 111 (2017) 260–263.

[108] M. Nascimento, M.S. Ferreira, J.L. Pinto, Temperature fiber sensing of lithium-ion batteries under different environmental and operating conditions, Appl. Therm. Eng. (2019) 1236–1243.

[109] T. Grandjean, A. Barai, E. Hosseinzadeh, et al., Large format lithium ion pouch cell full thermal characterisation for improved electric vehicle thermal management, J. Power Sources 359 (2017) 215–225.

[110] M. Parhizi, M.B. Ahmed, A. Jain, Determination of the core temperature of a lithium-ion cell during thermal runaway, J. Power Sources 370 (2017) 27–35.

[111] L.H.J. Raijmakers, D.L. Danilov, R.-A. Eichel, et al., A review on various temperature-indication methods for lithium-ion batteries, Appl. Energy 240 (2019) 918–945.

[112] C. Du, W.S. Zhang, L.M. He, et al., Measuring device for internal temperature of lithium ion battery and measuring method[P], Chinese Patent: CN102052976 A, https://patents.google.com/patent/CN102052976A/en, 2011-05-11. Available.

[113] A. Raghavan, P. Kiesel, L.W. Sommer, et al., Embedded fiber-optic sensing for accurate internal monitoring of cell state in advanced battery management systems part 1: cell embedding method and performance, J. Power Sources 341 (2017) 466–473.

[114] A. Ganguli, B. Saha, A. Raghavan, et al., Embedded fiber-optic sensing for accurate internal monitoring of cell state in advanced battery management systems part 2: internal cell signals and utility for state estimation, J. Power Sources 341 (2017) 474–482.

[115] A. Fortier, M. Tsao, N.D. Williard, et al., Preliminary study on integration of fiber optic bragg grating sensors in lithium-ion batteries and in situ strain and temperature monitoring of battery cells, Energies 10 (838) (2017) 1–11.

[116] M. Nascimento, S. Novais, M.S. Ding, et al., Internal strain and temperature discrimination with optical fiber hybrid sensors in lithium-ion batteries, J. Power Sources 410–411 (2019) 1–9.

[117] N.S. Spinner, C.T. Love, S.L. Rose-Pehrsson, et al., Expanding the operational limits of the single-point impedance diagnostic for internal temperature monitoring of lithium-ion batteries, Electrochim. Acta 174 (2015) 488–493.

[118] L.H.J. Raijmakers, D.L. Danilov, J.P.M. van Lammeren, et al., Sensorless battery temperature measurements based on electrochemical impedance spectroscopy, J. Power Sources 247 (2014) 539–544.

[119] L.H.J. Raijmakers, D.L. Danilov, J.P.M. van Lammeren, et al., Non-zero intercept frequency: an accurate method to determine the integral temperature of lithium-ion batteries, IEEE Trans. Ind. Electron. 63 (5) (2016) 3168–3178.

[120] R. Srinivasan, P.A. Demirev, B.C. Carhuff, Rapid monitoring of impedance phase shifts in lithium-ion batteries for hazard prevention, J. Power Sources 405 (2018) 30–36.

[121] R. Srinivasan, B.C. Carhuff, M.H. Butler, et al., Instantaneous measurement of the internal temperature in lithium-ion rechargeable cells, Electrochim. Acta 56 (2011) 6198–6204.

[122] B.G. Carkhuff, P.A. Demirev, R. Srinivasan, Impedance-based battery management system for safety monitoring of lithium-Ion batteries, IEEE Trans. Ind. Electron. 65 (8) (2018) 6497–6504.

[123] R. Schwarz, K. Semmler, M. Wenger, et al., Sensorless battery cell temperature estimation circuit for enhanced safety in battery systems, in: IECON 2015 - 41st Annual Conference of the IEEE Industrial Electronics Society, Yokohama, 2015, 001536-001541.

[124] J.P. Schmidt, S. Arnold, A. Loges, et al., Measurement of the internal cell temperature via impedance: evaluation and application of a new method, J. Power Sources 243 (2013) 110–117.

[125] J.G. Zhu, Z.C. Sun, X.Z. Wei, et al., A new lithium-ion battery internal temperature on-line estimate method based on electrochemical impedance spectroscopy measurement, J. Power Sources 274 (2015) 990–1004.

[126] H.P.G.J. Beelen, L.H.J. Raijmakers, M.C.F. Donkers, et al., A comparison and accuracy analysis of impedance-based temperature estimation methods for lithium-ion batteries, Appl. Energy 175 (2016) 128–140.

[127] S. Koch, K.P. Birke, R. Kuhn, Fast thermal runaway detection for lithium-ion cells in large scale traction batteries, Batteries 4 (16) (2018) 1–11.

[128] Z.R. Wang, Y. Yang, X. Tong, et al., Lithium-ion battery pack thermal runaway automatic alarming apparatus based on gas monitoring and monitoring method [P], Chinese Patent: CN108008083A, https://patents.google.com/patent/CN108008083A/en, 2018-05-08. Available:.

[129] S.R. Cummings, S.L. Swartz, N.B. Frank, et al., Systems and methods for monitoring for a gas analyte [P], U.S. Patent: US20180003685A1, https://patents.google.com/patent/US20180003685A1/en, 2018-01-04. Available:.

[130] S.L. Cummings, N. Swartz, Off-gas monitoring for lithium ion battery health and safety[R], in: Wright Patterson AFB: Power Sources Committee Meeting, 2017. Available: http://www.ndia.org/-/media/sites/ndia/divisions/manufacturing/documents/nexceris offgasmonitoring.ashx?la=en.

[131] S.R. Cummings, S.L. Swartz, N.B. Frank, et al., Lithium ion battery off-gas monitoring for battery health and safety[R], in: Florida: 47th Power Sources Conference, 2016. Available: https://nexceris.com/wp-content/uploads/Lithium-Ion-Battery-Monitoring-System-White-Paper.pdf.

[132] D. Hill, B. Gully, A. Agarwal, et al., Detection of off Gassing from Lithium-Ion batteries[A], IEEE Energytech[C], Cleveland, USA, 2013, pp. 142–149, 2013.

[133] M. Wenger, R. Waller, V.R.H. Lorentz, et al., Investigation of gas sensing in large lithium-ion battery systems for early fault detection and safety improvement[A], in: IECON 2014 - 40th Annual Conference of the IEEE Industrial Electronics Society[C]. Dallas, USA, 2015, pp. 5654–5659.

[134] I. Belharouak, Y.-K. Sun, J. Liu Li, $Ni_{1/3}Co_{1/3}Mn_{1/3})O_2$ as a suitable cathode for high power applications, J. Power Sources 123 (2) (2003) 247–252.

[135] F. Zhou, X. Zhao, J.R. Dahn, Impact of Al or Mg substitution on the thermal stability of $Li_{1.05}Mn_{1.95-z}M_zO_4$ (M = Al or Mg), J. Electrochem. Soc. 157 (2010) A798–A801.

[136] Y.-K. Sun, S.-T. Myung, B.-C. Park, et al., High-energy cathode material for long-life and safe lithium batteries, Nat. Mater. 8 (2009) 320–324.

[137] Y. Wu, A. Manthiram, High capacity, surface-modified layered $Li[Li_{(1-x)/3}Mn_{(2-x)/3}Ni_{x/3}Co_{x/3}]O_2$ cathodes with low irreversible capacity loss, Electrochem. Solid State Lett. 9 (2006) A221–A224.

[138] Y.-K. Sun, M.-J. Lee, C.S. Yoon, et al., The role of AlF_3 coatings in improving electrochemical cycling of Li-enriched nickel-manganese oxide electrodes for Li-ion batteries, Adv. Mater. 24 (2012) 1192–1196.

[139] Q. Wang, L. Feng, J. Sun, A multi-component additive to improve the thermal stability of $Li(Ni_{1/3}Co_{1/3}Mn_{1/3})O_2$-based lithium ion batteries, Energies 9 (2016) 424.

[140] L. Xia, S.-L. Li, X.-P. Ai, et al., Temperature-sensitive cathode materials for safer lithium-ion batteries, Energy Environ. Sci. 4 (2011) 2845–2848.

[141] C.-C. Lin, H.-C. Wu, J.-P. Pan, et al., Investigation on suppressed thermal runaway of Li-ion battery by hyper-branched polymer coated on cathode, Electrochim. Acta 101 (2013) 11–17.

[142] X.-B. Cheng, R. Zhang, C.-Z. Zhao, et al., Toward safe lithium metal anode in rechargeable batteries: a review, Chem. Rev. 117 (15) (2017) 10403–10473.

[143] G. Zheng, S.W. Lee, Z. Liang, et al., Interconnected hollow carbon nanospheres for stable lithium metal anodes, Nat. Nanotechnol. 9 (2014) 618–623.

[144] K. Liu, A. Pei, H.R. Lee, et al., Lithium metal anodes with an adaptive "solid liquid" interfacial protective layer, J. Am. Chem. Soc. 139 (2017) 4815–4820.

[145] M. Schmidt, U. Heider, A. Kuehner, et al., Lithium fluoroalkylphosphates: a new class of conducting salts for electrolytes for high energy lithium-ion batteries, J. Power Sources 97–98 (2001) 557–560.
[146] D.F. Liu, J. Nie, L.M. Zhuo, et al., New type of lithium poly(polyfluoroalkoxy) sulfonylimides as salts for PEO-based solvent-free electrolytes, J. Appl. Polym. Sci. 82 (8) (2001) 1882–1885.
[147] D.H.C. Wong, J.L. Thelen, Y. Fu, et al., Nonflammable perfluoropolyether-based electrolytes for lithium batteries, Proc. Natl. Acad. Sci. U.S.A. 111 (2014) 3327–3331.
[148] H.Q. Pham, H.-Y. Lee, E.-H. Hwang, et al., Non-flammable organic liquid electrolyte for high-safety and high-energy density Li-ion batteries, J. Power Sources 404 (2018) 13–19.
[149] J. Wang, Y. Yamada, K. Sodeyama, et al., Fire-extinguishing organic electrolytes for safe batteries, Nat. Energy 3 (2018) 22–29.
[150] Z. Zeng, V. Murugesan, K.S. Han, et al., Non-flammable electrolytes with high salt-to-solvent ratios for Li-ion and Li-metal batteries, Nat. Energy 3 (2018) 674–681.
[151] J. Pires, A. Castets, L. Timperman, et al., Tris(2,2,2-trifluoroethyl) phosphite as an electrolyte additive for high-voltage lithium-ion batteries using lithium-rich layered oxide cathode, J. Power Sources 296 (2015) 413–425.
[152] Z. Jin, H. Gao, C. Kong, H. Zhan, Z. Li, A novel phosphate-based flame retardant and film-forming electrolyte additive for lithium ion batteries, ECS Electrochem. Lett. 2 (2013) A66–A68.
[153] T. Han, B. Khalighi, E.C. Yen, et al., Li-ion Battery pack thermal management: liquid versus air cooling, J. Therm. Sci. Eng. Appl. 11 (2) (2019), 021009.
[154] M. Parhizi, A. Jain, Analytical modeling and optimization of phase change thermal management of a Li-ion battery pack, Appl. Therm. Eng. 148 (2019) 229–237.
[155] S. Wilke, B. Schweitzer, S. Khateeb, et al., Preventing thermal runaway propagation in lithium ion battery packs using a phase change composite material: an experimental study, J. Power Sources 340 (2017) 51–59.
[156] L. Song, H. Zhang, C. Yang, et al., Thermal analysis of conjugated cooling configurations using phase change material and liquid cooling techniques for a battery module, Int. J. Heat Mass Transf. 133 (2019) 827–841.
[157] W.X. Wu, S.F. Wang, W. Wu, et al., A critical review of battery thermal performance and liquid based battery thermal management, Energy Convers. Manag. 182 (2019) 262–281.
[158] J. Kim, J. Oh, H. Lee, Review on battery thermal management system for electric vehicles, Appl. Therm. Eng. 19 (2019) 192–212.
[159] A.R.M. Siddique, S. Mahmud, B. van Heyst, A comprehensive review on a passive (phase change materials) and an active (thermoelectric cooler) battery thermal management system and their limitations, J. Power Sources 401 (2018) 224–237.
[160] M. Al-Zareer, I. Dincer, M.A. Rosen, A review of novel thermal management systems for batteries, Int. J. Energy Res. 42 (10) (2018) 3182–3205.
[161] H.Q. Liu, Z.B. Wei, W.D. He, et al., Thermal issues about Li-ion batteries and recent progress in battery thermal management systems: a review, Energy Convers. Manag. 150 (2017) 304–330.
[162] W.A. Hermann, A. Prilutsky, V.H. Mehta, Battery pack enclosure with controlled thermal runaway release system, U.S. Patent: US8277965B2, https://patents.google.com/patent/US8277965B2/en, 2012-10-2. Available.
[163] W.A. Hermann, Cell separator for minimizing thermal runaway propagation within a battery pack, U.S. Patent: US8367239B2, https://patents.google.com/patent/US8367239B2/en, 2013-02-05. Available.
[164] W.A. Hermann, S.I. Kohn, V.H. Mehta, et al., Thermal barrier structure for containing thermal runaway propagation within a battery pack, U.S. Patent: US8541126B2, https://patents.google.com/patent/US8541126B2/en, 2013-09-24. Available.
[165] W.A. Hermann, S.I. Kohn, E.M. Berdichevsky, et al., Increased resistance to thermal runaway through differential heat transfer, U.S. Patent: US20100151308A1, https://patents.google.com/patent/US20100151308A1/en, 2010-06-17. Available:.
[166] E.M. Berdichevsky, P.D. Cole, A.J. Hebert, et al., Mitigation of propagation of thermal runaway in a multi-cell battery pack, U.S. Patent: US7433794B1, https://patents.google.com/patent/US7433794B1/en, 2008-10-07. Available:.
[167] P.D. Rawlinson, A.P. Clarke, H.L. Gadhiya, et al., System for absorbing and distributing side impact energy utilizing an integrated battery pack, U.S. Patent: US8702161B2, https://patents.google.com/patent/US8702161B2/en, 2014-04-22. Available:.
[168] L. Chow, Battery pack, U.S. Patent: US20110091749A1, https://patents.google.com/patent/US20110091749A1/en, 2011-04-21. Available:.
[169] S. Hore, J. Fetzer, R. Angerbauer, et al., Apparatus and Method for Providing Safety Measures during Gas Release from a Vehicle Battery and Installation Space for a Vehicle Battery, U.S. Patent: US9269936B2, 2016-02-23. Available, https://patents.google.com/patent/US9269936B2/en.